Biofabrication 2013

El Paso, TX

Nov. 3 – Nov.6, 2013

Abstracts

Index

POSTERS

The Third Strategy in Tissue Engineering: Design, Fabrication and Material Testing of Concentric Interlockable Microscaffold (Lockyballs) with Enhanced Material Properties for Rapid *In Situ* 3D Bone Tissue Biofabrication

Paulius Danilevicius[2], Anna Mitraki[2], Maria Chatzinikolaidou[2], Frederico D.A.S. Pereira[1], Rodrigo A. Rezende[1], Rafael Rocha Mattazio[1], Pedro Y. Noritomi[1], Jorge V.L. da Silva[1], Maria Farsari[2], Vladimir Mironov[1,2]

[1]Center for Information Technology Renato Archer (CTI), Campinas, SP, Brazil; [2]FORTH-IESL, University of Crete, Heraklion, Crete, Greece

Introduction

The bottom-up modular directed tissue self-assembly and solid scaffold based approach are two distinct premises in tissue engineering (1). There is a growing consensus that a third strategy based on the integration of a directed tissue self-assembly approach with a conventional solid scaffold-based approach could be a potential optimal solution (1,2). We recently introduced a concept of tissue spheroids encaged into interlockable microscaffolds or lockyballs which combines advantages of both main distinct approaches in tissue engineering as a variant of desirable third strategy and as a new technological platform for rapid *in situ* 3D tissue biofabrication (3). We report here the design, fabrication and material testing of second generation of interlockable microscaffold or lockyballs for rapid *in situ* biofabrication of bone tissue with material properties enhanced by concentric geometrical design.

Materials and Methods

Concentric interlockable microscaffolds or lockyballs have been designed using preliminary design studies using finite element analysis software. Lockyballs have been fabricated using two photon polymerization of organically modified photo-sensitive biomaterials. Scanning electron microscopy has been used to study morphology and geometry of fabricated lockyballs. Material properties of lockyballs have been tested using parallel plates compression test (MicroSquisher, Cellscale Inc, Toronto, Canada). The bulk cube and non-concentric lockyballs fabricated by the same method from the same polymer have been used as a control. The lockyballs have been cellularized using micromolded non-adhesive agarose hydrogel. Biocompatibility of concentric lockyballs has been estimated in vitro using early passages of the mouse pre-osteoblastic cell line MC3T3-E1 with proven osteogenic capacities. Quantitative data has been statistically analyzed.

Results and Discussion

Concentric interlockable microscaffold has been designed and fabricated using two photon polymerization (Fig.1). The lockyballs have been interlocked using mechanical loading. Estimation of material properties of concentric lockyballs are 25-30 stronger then material properties of lockyballs of non-concentric design and are very close to material properties of bulk cube from the same materials. It has been demonstrated that concentric design of lockyballs not only enhances their material properties but also permits their effective cellularization in micromolded non-adhesive agarose hydrogel. Viability tests demonstrated high level of biocompatibility of fabricated lockyballs.

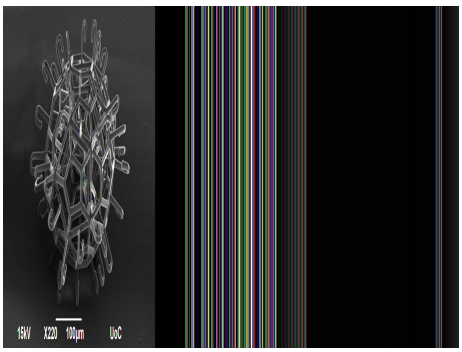

Figure 1. Scanning electron microscopy of interlockable concentric microscaffold (lockyballs) with enhanced materials properties fabricated by two phton polymerization from photo-sensitive biomaterials

Conclusions

By changing geometrical design of lockyballs it is possible to achieve desirable level of material properties of lockyballs comparable with material properties of bulk material. Tissue spheroids encaged in mechanically enhanced concentric intrelockable microscaffold do not compromise their capacity for tissue fusion and additionally have enhanced material properties and capacity for rapid in situ biofabrication into 3D tissue constructs using lockyballs-mediated mechanical interlocking. Thus, interlockable microscaffold or lockyballs represent a third strategy in tissue engineering which allows to combine advantages of two main distinct premises in tissue engineering - conventional solid scaffold-based approach with bottom-up modular directed tissue self-assembly based approach.

References

1. Kachouie N. et al. Organogenesis, 2010, 6 (4): 234-244.
2. Billiet T. et al. Biomaterials, 2012, 33 (26): 6020-6041.
3. Rezende R. et al. Virtual and Physical Prototyping, 2012, 7(4): 287-301.

Acknowledgements

study was partly funded by Brazilian funding agencies CNPq and FAPESP and by FP7 Marie Curie ITN program TopBio.

Bioprinting with Decellularized Extracellular Matrix and its Effectiveness for Chondrogenic Differentiation

Jinah Jang[1], Falguni Pati[2], Tae-Ha Song[2], Sung Won Kim[3] and Dong-Woo Cho[2,*]

[1]Division of Integrative Bioscience and Biotechnology, POSTECH, Pohang, Kyungbuk, South Korea
[2]Department of Mechanical Engineering, POSTECH, Pohang, Kyungbuk, South Korea
[3]Department of Otolaryngology-HNS, The Catholic University of Korea, Seoul, Korea

* Corresponding author: dwcho@postech.ac.kr

Introduction

Maintaining of biomechanical properties and material composition of native extracellular matrix (ECM) are critical cues to create native environment for tissue regeneration due to its specificity depending on the target tissues. Thus, Decellularized ECM (dECM) have been introduced as a promising material because of its biomimetic structural and material compositions. Herein, we would like to show the 3D cell-laden construct like a hybrid structure of bioskeleton (PCL) and bio ink (dECM) to create native 3D microenvironment with supportive mechanical property of large volume construct and verify the effect of dECM on the differentiation of human turbinate tissue-derived mesenchymal stem cells to the desired lineage and its ability to let the 3D construct form the desired tissue by utilizing 3D cell printing technology.

Materials and Methods

dECM solution were prepared for cell printing. It mixed with cells and printed with 3D polymeric framework by in-house 3D cell printing equipment called Multi-head Tissue/Organ Printing System. The final concentration of dECM and COL gel were 3%. Rheological properties of dECM hydrogel were investigated. After 3 days and 15 days culture, we demonstrated the site appropriate tissue formation by RT-PCR and immunofluorescence staining methods.

Results and Discussion

dECM solution could be a powerful bio ink for 3D cell printing because crosslinking occurred at neutral pH and 37°C environment without any harmful crosslinker. Moreover, the flow viscosity of 3% dECM solution has reasonable value for dispensing through the nozzle, and its viscoelastic modulus shows similar value with that of native cartilage tissue. In particular, dECM derived from cartilage shows the highest expression level of SOX9 as well as PTK2 and Integrin β1, which are the representative marker for cell signaling and adhesion, respectively. 3D cell-laden dECM/PCL construct were cultured for 15days and verify chondrogenic marker gene expression, including SOX9, Collagen type II. In conclusion, chondrogenic differentiation and synthesis its specific ECM were increased when dECM was used as a bio-ink.

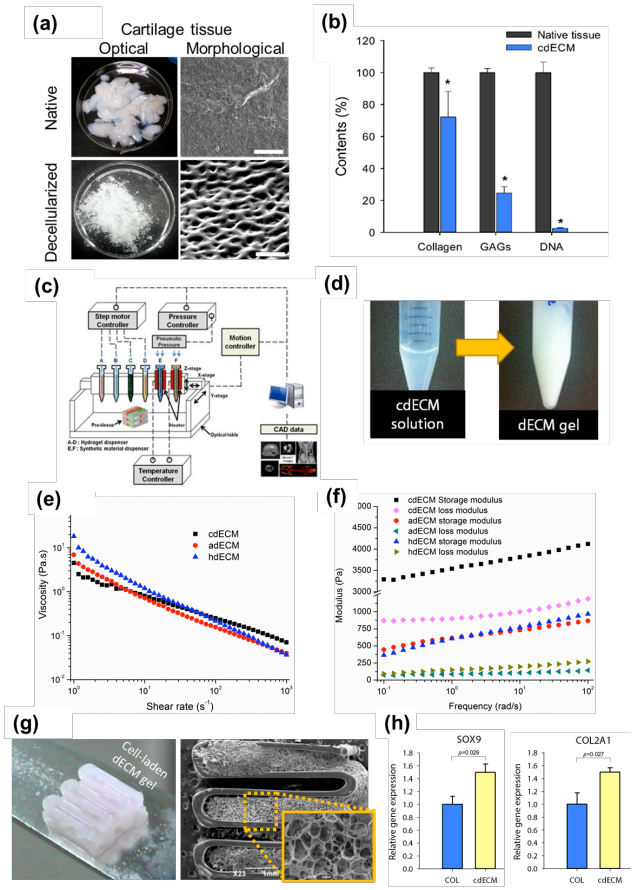

Figure 1.(a) Morphological analysis and (b) biochemical analysis before and after decellularization. (c) Schematic of apparatus for 3D cell printing and (d) dispensible dECM hydrogel before and after crosslinking. (e) Flow viscosity and (f) shear modulus of dECM. (g) Optical and SEM images of fabricated 3D cell-laden construct. (h) Marker gene expression on each materials after 14days .

Acknowledgement

This work was supported by the National Research Foundation of Korea (NRF) grant funded by the Korea government (MSIP) (No. 2010-0018294).

Engineering an Implantable Liver Tissue Equivalent based on Perfusion Culture of Cellular Aggregates in Scalable Three-dimensional Scaffold

Yuan PANG[1, *], Yohei HORIMOTO[2], Toshiki NIINO[1], Yasuyuki SAKAI[1]
[1] Institute of Industrial Science, University of Tokyo, Komaba 4-6-1, Meguro-ku, Tokyo 153-8505, Japan
[2] Graduate School of Engineering, Shibaura Institute of Technology, Shibaura 3-9-14, Minato-ku, Tokyo 108-8548, Japan

Introduction

To sustain the homeostasis of human body at least 20-30% of hepatic functions should be retained, which also indicates the necessary volume for implantable liver tissue is around 20-30% of real liver organ size around 500 cm^3 in volume [1]. However, to data, a 500 cm^3-scale liver tissue equivalent with a comparably high cell density and functionality for implantation has not yet been successfully achieved. To point out, the essential problems that liver tissue engineering still facing are 1) sufficient mass transfer to support tissues of high per-volume-functionality matching *in vivo* condition; and 2) adequate cell number to achieve a clinically relevant size at least 500 cm^3-scale. We herein proposed a new methodology of "integration of bottom-up and top-down technologies" towards construction of large size liver tissue with a clinically significant mass, based on assembling cellular aggregates in a newly fabricated three-dimensional (3D) scaffold.

Materials and Methods

The scaffold was designed based on the real liver structure, which comprised of 43 chambers for cell culture assembled on three layers (CAD model is shown in Fig. 1a). 12 chambers were posited on the 1st and the 3rd layer, and 19 chambers on the 2nd layer, promising the whole construct to obtain a symmetric outer shape. The construct of 43 chambers can be further arranged again in the same way of pattern to finally achieve a structure 500 cm^3 in volume. The cell culture chambers were designed to be a cylinder of hexagon section, which was about 0.27 cm^3 in volume. Interconnected flow-channels were designed to deliver culture medium independently to each of the chambers. The diameter of each flow channel was calculated based on Murray's law and Hagen-Poiseuille equation to ensure the same pressure drop of the flow to each chamber. The scaffold arranged at the first scale of which the volume was 11.63 cm^3 was fabricated using Nylon-12 due to its high mechanical strength (Fig. 1b).

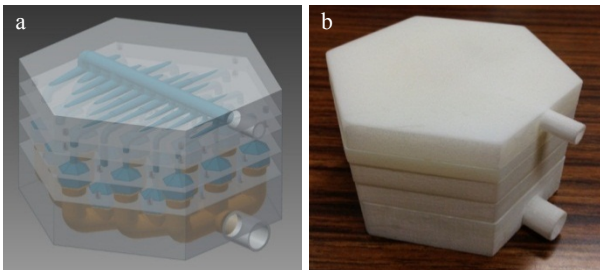

Fig. 1 CAD design of the scaffold (a) and fabricated scaffold (b).

Cellular aggregates were prepared by co-culturing human hepatoma Hep G2 cells and TMNK-1 cells in the PDMS-based microwell device. Aggregates were collected from the microwells after formation, mixed with PLLA fiber suspension, and transferred to the scaffold for perfusion culture. Culture medium was replaced every 24 h.

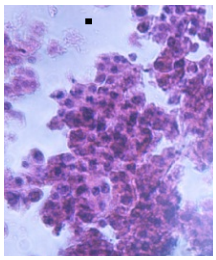

Fig. 2 H&E stained cross section of aggregates after 10 days perfusion. Scale bar: 100 μm

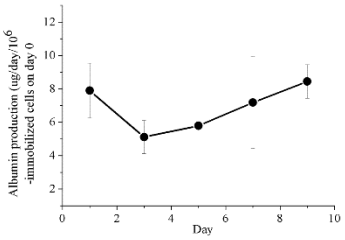

Fig. 3 Human albumin production of aggregates during 10 days perfusion.

Results and Discussion

After 10 days of perfusion culture in the scaffold, cell viability was still high according to H&E staining of cross section (Fig 2). The albumin production of the co-cultured aggregates had a slight drop at the beginning of perfusion, which was considered due to the unstable flow condition usually happens right after the setup of a perfusion culture. When the perfusion became stable, the albumin production kept increasing throughout the whole 10 days of culture (Fig. 3). The glucose consumption also decreased till day 3 and then started to steadily grow till day 7 and became stable. The gradually increased albumin production, glucose consumption and high cell viability during 10 days of perfusion culture demonstrated that such 3D scaffold consisting chambers for cell culture and independent flow channels for medium delivery was essential to the cell growth and function.

Conclusions

The first attempt on approaching to implantable liver tissue equivalent by integration of "bottom-up" and "top-down" concepts was proved successful, with resolving the insufficient mass transfer simultaneously from micro- and macro-scale. The scalable design of the scaffold itself exhibited the potential to be further scaled up towards a clinically-relevant size of 500 cm^3 in volume.

Reference

[1] Sakai Y, Huang H, Hanada S, Niino T. *Biochem. Eng. J.* 2010, 48, 348-361.

* Corresponding author: pangyuan@iis.u-tokyo.ac.jp

Bioprinting a Hybrid Scaffold Containing Human Placenta Derived Extracellular Matrix

Xuan Guo, Aleksandr Kaplunovsky, Raihana Zaka, Robert J. Hariri, Wolfgang T. Hofgartner, Mohit B. Bhatia
Celgene Cellular Therapeutics, 33 Technology Drive, Warren, NJ 07059, USA

Introduction

Recently, a number of synthetic biomaterials have been bioprinted to three dimensional (3D) scaffolds for tissue engineering applications. However, synthetic scaffolds alone lack biological cues to guide tissue regeneration. Therefore, the objective of this study was to incorporate a human placenta derived extracellular matrix (ECM) [1] into a bioprinted synthetic scaffold to create hybrid scaffolds. Previously we have developed a process to isolate ECM from human placenta. The resulted ECM contains 60~70% (dw) collagen, ~ 25% elastin and 1-2% of glycosaminoglycans, fibronectin and laminin [2]. In this study we are developing bioprinting techniques to incorporate human placenta ECM into polycaprolactone (PCL), a synthetic material, to fabricate hybrid scaffolds.

Materials and Methods

Two approaches have been developed to generate ECM hybrid scaffolds. ECM used for both approaches was isolated from human placenta according to a previously established procedure [2].

In the first approach, PCL (Mn 45,000, Sigma) was first fabricated as a 3D scaffold with a bioprinter (EnvisionTEC). The ECM was then applied to both sides of the bioprinted PCL scaffolds and subjected to a dehydration process. The resulted hybrid PCL-ECM scaffolds were seeded with Placenta Derived Adherent Cells (PDAC®) cells at 12,500/cm^2 to evaluate scaffold biocompatibility.

In a separate method, PCL and ECM were both printed into a layered scaffold. In each layer of the scaffold, PCL was first printed, then ECM mixed with 0.5% alginate hydrogel containing 1 million/mL PDAC® cells were printed to fill the gaps in between the PCL lines. Five layers were printed and crosslinked with $CaCl_2$ solution to generate the hybrid scaffolds.

For both types of the scaffolds, Calcein AM staining and MTS assay were performed to evaluate cell viability and proliferation on the scaffolds over the culture period.

Results and Discussion

Using the dehydration method, ECM was incorporated on both sides of bioprinted PCL scaffolds, forming a hybrid scaffold. Good integration was seen between PCL and ECM. PDAC® cells seeded on the hybrid scaffolds showed good viability during the 8 day culture period, as indicated by Calcein staining. MTS assay further shows cell number increased from 2115 ± 424 to 22764 ± 5632 per scaffold during 8 days, suggesting that PCL-ECM hybrid scaffolds supported PDAC® cells attachment and growth.

Using the bioprinting method, hybrid scaffolds were generated, and they maintained an intact structure during culture (Figure 1). PCL provided a good structural support for the ECM hydrogels, allowing to build the 3D constructs. A good cell distribution was found throughout the depth of the scaffolds during culture. PDAC® cells survived the printing process. They spread around the ECM, and proliferated in the bioprinted hybrid scaffolds during the culture, as evidenced by Calcein staining (Figure 1). MTS data also show a 3.72 ± 0.25 fold increase in cell number for the scaffolds in 7 days, suggesting these hybrid scaffolds supported PDAC® cell growth.

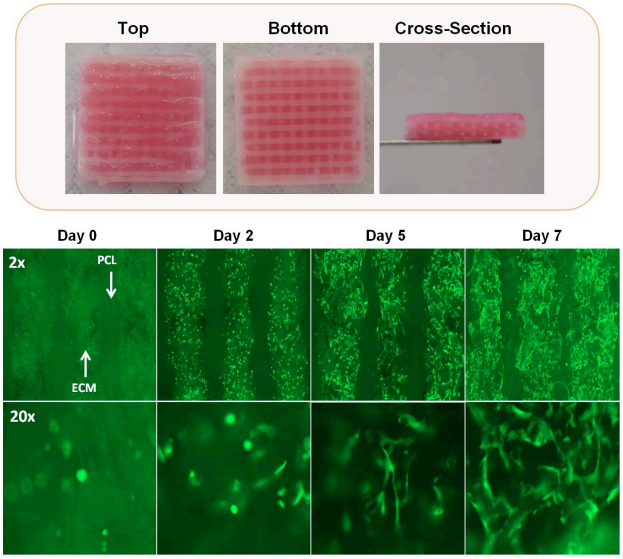

Figure 1. Bioprinted PCL-ECM hybrid scaffolds support PDAC® cell proliferation

Conclusions

In this work, we fabricated hybrid scaffolds by combining a synthetic biomaterial, PCL, and a natural material, placenta derived ECM using bioprinting technology. Two methods, dehydration and bioprinting methods, have been developed to fabricate the hybrid scaffolds. In both methods, we found good integration between PCL and ECM. Bioprinted PCL of controlled fiber size formed a stable network to support structure of the hybrid scaffolds. Additionally, placenta derived ECM provided biological cues that enhanced PDAC® cell attachment, spreading, and proliferation in these hybrid scaffolds. The results demonstrate great potential of bioprinting technique for fabrication hybrid scaffolds involving the use of both synthetic and placenta derived natural materials for tissue engineering applications.

References

1. Bhatia MB, Wounds 20, 29, 2008
2. Press BH, et al. Poster, TERMIS NA, 2011

Bio-3D Printing: Challenges and Opportunities

Wei Sun, Ph.D.
Albert Soffa Chair Professor, Drexel University; Philadelphia, PA 19104, USA
1000plan Chair Professor, Tsinghua University, Beijing, China

Abstract:

For millions of years, cells have been thought of as Nature's building blocks that make living organisms what they are. Advance in 3D Printing has emerged an interdisciplinary field of Bio-3D Printing in which cells, biomaterials and other biologics can be used as building blocks for construction of personalized 3D structures or in vitro biological models through additive manufacturing processes. Bio-3D Printing provides a vital tool to the field of tissue science and engineering, personalized medicine, disease pathogeneses study, drug testing and discovery, cell/tissue-on-a-chip, and cell and organ printing. This presentation will report our recent work on Bio-3D Printing, focusing on the printing process, modeling on process-induced cell injury, and its applications, along with a review on recent development of cell printing as an emerging field as well as the enabling cell printing techniques. Challenges and opportunities of Bio 3D Printing for additive manufacturing, biomaterials and biology will also be discussed.

Biological comparison of RP scaffolds made from either PCL, PLDLLA and 300PEOT55PBT45

WJ Hendrikson[1], CA van Blitterswijk[1], J Rouwkema[2], L Moroni[1]

[1] Departement of Tissue Regeneration, University of Twente, Netherlands
[2] Departement of Biomechanical Engineering, University of Twente, Netherlands

Introduction

In tissue engineering, the goal is to regenerate and/or restore malfunctioning tissue. In this aspect, a scaffold provides a temporary structure for cells to attach to and form tissue. Common biomaterials used for scaffolds are ceramics and polymers. While ceramics are known to have excellent osteo-inductive and osteo-conductive properties, polymers do not – or only marginally – possess these properties. However, polymers can be processed with various techniques, therefore allowing for any overall scaffold shape. One such technique is Rapid Prototyping (RP) with which highly controllable and reproducible scaffolds can be made. The biomaterial of the scaffold can elicit a specific biological response in-vitro and/or in-vivo when implanted. Therefore, it is important to know how cells respond to multiple scaffold materials, in order to select the most optimal polymer for a specific application. Cellular behavior on multiple materials have been described in literature [1-3], but direct comparisons between materials with the same architectural scaffold are scarce. RP scaffolds were fabricated from PCL, PLA and PEOT/PBT. hMSCs were seeded in these scaffolds and exposed to basic, osteogenic and chondrogenic medium for 28 days.

Materials and Methods

Scaffolds of 8 mm were punched out from larger blocks obtained through 3D fiber deposition. 300PEOT55PBT45 (PolyVation), PCL (Mw 65.000, Sigma Aldrich) and Poly L-DL-Lactic Acid 80/20 (Purac) were used as biomaterial. Collagen type I coated scaffolds were seeded with hMSCs (P3, 500.000/scaffold) and kept in culture for 7 days in proliferative medium (basic + bFGF) followed by 28 days in either basic (α-MEM + 10% FBS + 1 % L-Glutamin + 0.2 mM ascorbic acid + 100 U/ml penicillin + 10 ug/ml streptomycin), osteogenic (basic + dexamethasone) or chondrogenic medium (D-MEM + 100 U/ml penicillin + 10 ug/ml streptomycin + 0.2 mM ascorbic acid + ITS-mix + sodium pyruvaat + fresh dexamethasone and TGF-b3). Each timepoint (7, 14 and 28 days), three scaffolds were harvested for DNA, ALP and GAG quantification and one for cell localization – through Methylene blue and SEM – and ALP staining.

Results and Discussion

Irrespective of the polymer, the amount of ECM formed was highest when exposed to osteogenic medium while chondrogenic medium had the least ECM. Although differences are small, SEM images showed slightly more ECM in the 300/55/45 scaffolds compared to PCL and PLDLLA. Methylene blue showed a slightly higher cell density on the lower part of the scaffold, likely due to gravity during cell seeding of the scaffolds. Furthermore, the rounded cell shape seen in the chondrogenic medium suggest hMSCs were going into the chondrogenic lineage. ALP staining showed differences between the materials. In PLDLLA it was only strong for day 28 in osteogenic medium. PCL had a strong staining for day 14 in osteogenic and day 28 in osteogenic and chondrogenic medium. 300/55/45 had a weak staining for basic medium in all time points while it was strong for day 14 and 28 in osteogenic medium. In chondrogenic medium, the staining was medium to strong for all timepoints. To quantify and confirm these observations, scaffolds are currently being cultured for ALP, DNA and GAG quantification.

Table 1. ALP staining results

	Basic			Osteogenic			Chondrogenic		
	T1	T2	T3	T1	T2	T3	T1	T2	T3
PEOT/PBT	-+	-+	-+	+	++	++	+	+	+
PCL	-	-+	-	-+	++	+	-+	-	++
PLDLLA	-	-	-+	-	-	++	-	+	-

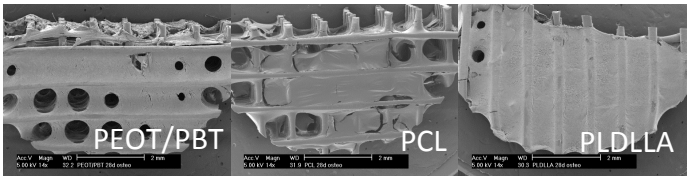

Figure 1. SEM figures of scaffolds cultured in osteogenic medium for 28 days. (scalebar is 2 mm)

Conclusions

These results show that the biological response of hMSCs in seeded scaffolds, varies with the polymer used. Although ALP, DNA and GAG still has to be performed to confirm the results. ALP staining suggests that 300/55/45 triggers the osteogenic differentiation of hMSCs. The cell shape from scaffolds in chondrogenic medium, indicates chondrogenic differentiation of the hMSCs.

Acknowledgements

We would like to acknowledge funding from the Netherlands Institute of Regenerative Medicine, contract grant number: FES0908.

References

1. Shor, L., et al., Biofabrication, 2009
2. Duan, B., et al., Acta Biomaterialia, 2010
3. Woodfield, T.B.F., et al., Biomaterials, 2004

Topology Optimization of Tissue Scaffolds for 3D Printing

Che-Cheng Chang1, Shiwei Zhou, Qing Li

Introduction

Design and control of microstructure signifies a major challenge in the development of porous tissue scaffolds. Past studies have established a range of porosity requirements for cell survival and proliferation [1]. Numerous biofabrication techniques have been developed to date to produce the required scaffold structures, 3D printing in particularly is one of the techniques used for such purpose [2, 3]. In the recent years, topology optimization methods are also applied to this field of research in an effort to determine the best possible microstructures with desirable stiffness, diffusivity and permeability [4, 5]. However, the concept of an ideal tissue scaffold has yet been fully realized, partly because the model quality of common topology optimization methods do not meet the manufacturing requirements, and partly due to the technical limitations in current fabrication techniques to accurately build the ideal microscopic details.

Methods

To resolve the design realization issue, this study develops a topology optimization method using isosurface modeling technique, which allows the construction of clearly defined optimal microstructure suitable for biofabrication purpose (e.g. in direct 3D-printable format). This method creates computational models with an implicitly defined level set and an explicitly defined isosurface, on which the simulation and design optimization are performed in a more boundary-accurate fashion. The models are optimized based on the level set method to maximize the effective material properties.

Results and Discussion

A range of optimal microstructures with various combinations of effective diffusivity and bulk modulus have been thereafter defined in isosurface form (Fig. 1). A smooth Pareto front is also generated. The results show that both the maximum diffusivity model and the maximum bulk modulus model cannot be physically fabricated due to phase discontinuity, otherwise all intermediate models may be considered feasible candidates. With the distinct definition of the surface boundary, these results help clarify the geometric features of the optimal microstructures and clear some speculations raised by the past density-based topology optimization studies. In addition, the isosurface models and solutions are generated in a triangulated form equivalent to the stereolythography format, conforming to the rapid prototype standard, making the direct exportation to the 3D printable format possible without the need of further processing or human interpretation.

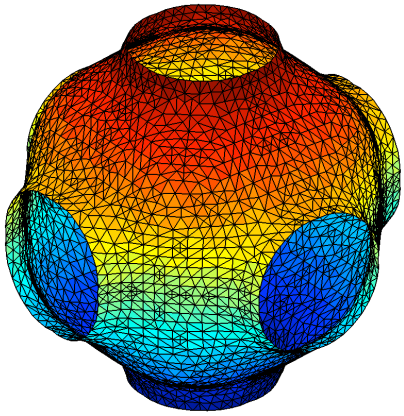

Figure 1. The unit-cell representation of the microstructure (void phase) with optimal diffusivity and bulk modulus.

Conclusions

This study is successful in bridging the gap between topology optimization and biofabrication through isosurface modeling. The proposed technique is therefore recommended for the design optimization of products such as porous tissue scaffolds that require 3D printing and rapid prototyping.

References

[1] S. Rajagopalan and R.A. Robb, Schwarz meets Schwann: Design and fabrication of biomorphic and durataxic tissue engineering scaffolds, Medical Image Analysis, 10(5), 693-712, 2006.

[2] C.E. Wilson, J.D. de Bruijn, C.A. van Blitterswijk, A.J. Verbout and W.J. Dhert, Design and fabrication of standardized hydroxyapatite scaffolds with a defined macro-architecture by rapid prototyping for bone-tissue-engineering research, J Biomed Mater Res A, 68(1), 123-32, 2004.

[3] F.P.W. Melchels, B. Tonnarelli, A.L. Olivares, I. Martin, D. Lacroix, J. Feijen, D.J. Wendt and D.W. Grijpma, The influence of the scaffold design on the distribution of adhering cells after perfusion cell seeding, Biomaterials, 32(11), 2878-2884, 2011.

[4] Y. Chen, S.W. Zhou and Q. Li, Computational design for multifunctional microstructural composites, International Journal of Modern Physics B, 23(6-7), 1345-1351, 2009.

[5] Y. Chen, S. Zhou, J. Cadman and Q. Li, Design of cellular porous biomaterials for wall shear stress criterion, Biotechnology and Bioengineering, 107(4), 737-746, 2010.

Additive Tissue Manufacturing for Soft Tissue Interfaces with a focus on Breast Reconstruction; combining computer aided design and manufacturing with tissue engineering strategies

Dietmar Hutmacher

QUT Chair in Regenerative Medicine| Institute of Health and Biomedical Innovation, Queensland University of Technology, 60 Musk Avenue, Kelvin Grove QLD 4059, Australia

Abstract

Additive Tissue Manufacturing for Soft Tissue Interfaces with a focus on Breast Reconstruction; combining computer aided design and manufacturing with tissue engineering strategies

Breast cancer is a major cause of illness for women. Following tumour resection, breast reconstruction is undertaken for cosmetic and psychological reasons. Reconstruction using silicone-based implants leads to complications such as formation of a rigid fibrous tissue surrounding the implant giving a spherical and unnatural appearance to the breast. Reconstruction using autologous tissue is associated with donor site morbidity, tissue resorption and necrosis. It has been hypothesised that these problems may be overcome with a tissue engineering approach. However, most large volume tissue engineering scaffolds develop a necrotic core due to inefficient nutrient diffusion. This project proposes a novel method having a combination of perfusable channels within a patient-specific scaffold that will allow continuous provision of nutrients and oxygen to the cells at the core of the scaffold and significantly lowers the possibility of cell death due to hypoxia. In addition, the lack of functional integration between tissue-engineered constructs (TEC's) and surrounding host tissues is a critical barrier, limiting the effectiveness and clinical translation of current soft tissue interface graft technologies. The overarching goal of this Hans Fischer Senior Fellowship research programme is to address this challenge through the development of highly adaptable platform technologies that enable the engineering of stronger interfaces between TEC's and the extracellular matrices that are distinct to particular clinical conditions. Through this project, an international network spanning scientists, engineers, clinicians, industry and government will be established to accelerate the pace of regenerative medicine research targeting reconstruction of complex soft tissue interface defects and abnormalities. Key outcomes of research program will deliver innovative new strategies for Additive Tissue Manufacturing for Soft Tissue Interfaces whilst contributing to the education a new generation of bioengineers, clinician scientists and tissue engineers with a strong international profile.

Gradient Pattern with Sinusoidal waves (GPS) for investigation of cell alignment induced by pseudo-three dimensional cell microenvironment

Sung Jea Park, Moon hee Na, and Dong Sung Kim*
Department of Mechanical Engineering, Pohang University of Science and Technology (POSTECH), South Korea

Introduction

In vivo three-dimensional (3D) micro-environment occurring in the cell-extracellular (ECM) interactions affects the cell behaviors, such as adhesion, alignment, migration, proliferation and differentiation [1,2]. Several types of micropatterns were developed to mimic the *in vivo* microenvironment for studying the cell behaviors, however, they were limited to those with the two dimensional (2D) structures having sharp edges, a sudden height change and a restricted height. Though such 2D micropatterns could facilitate cell behaviors, e.g., alignment, the effect induced by 3D microenvironments could not be mimicked. Therefore, we need to develop a pseudo-3D microenvironment based on the pattern with a sufficient and smooth variation of the height. For achieving such pseudo-3D microenvironment in form of groove-pattern, we developed the gradient patterns with sinusoidal waves (GPS) through LIGA (German acronym for LIthographie, Galvanoformung and Abformung, or lithography, electroforming and molding in English). The step-gradually altered periods enable us to perform the cell culture experiments on different patterns in the same condition and to facilitate the observation of cell behaviors on a single substrate. The present study addresses the influence of GPS, the proposed pseudo-3D microenvironment, on the alignment of osteosarcoma MG63 cells and fibroblast NIH3T3 cells. The present investigation is focused on two issues: (1) effects of GPS groove shapes (period and amplitude) on cell alignments and (2) relationship of sizes between cells and grooves.

Materials and Methods

Two different types of GPS having amplitudes (A) of 10 and 20 μm were designed to have step-gradient periods (λ) of 20, 40, 80 and 160 μm. It is noted that the groove walls with A of 20 μm is steeper than those with A of 10 μm and the size of the grooves is similar or larger than cell sizes (MG63: ~40 μm, NIH3T3: ~15 μm). The GPS patterns with polystyrene (PS) were replicated through the hot embossing process using the nickel mold inserts fabricated by deep X-ray lithography (DXRL) followed by electroforming process. *In vitro* cell culturing of MG-63 and NIH3T3 cells was performed to evaluate the cell alignments on the replicated PS GPS. The cells were incubated for 4 h and 24 h before the staining. DAPI and Phalloidin staining of the cells were carried to highlight the cell alignment as shown in Fig. 1(b). For the quantification, we considered that the cells were aligned if satisfying the following conditions: (1) the length ratio between of major axis and minor one of the cell was larger than two and (2) the major axis was oriented within ±15˚ of the groove direction of GPS.

Results and Discussion

The cell alignment was influenced by changing the shapes of the grooves as shown in Fig.1 (a). As λ was decreased and A was increased, the alignment of cells was improved because the steepness of the groove walls increased. From the regression analysis of the cell alignment data, it was revealed that the alignment was more-dominantly affected by λ than A. It could be concluded that the steepness determined the alignment of cells.

The cell alignment was also affected by the size relationship between the cells and GPS grooves as shown in Fig.1 (a). The large cells (MG63 cells) recognize the groove wall more-steeply compared with the small cell (NIH3T3). Due to the different recognition about the wall steepness, MG63 cells tend to be more aligned than NIH3T3. Interestingly, in the groove pattern with λ of 20 μm and A of 20 μm, NIH3T3 cells alignment was decreased compared with the alignment on groove pattern with λ of 20 μm and A of 10 μm though it had steeper walls. The cells in the groove were expanded to the perpendicular direction of the groove due to spatial margin between groove and cell (Fig.1(c)).

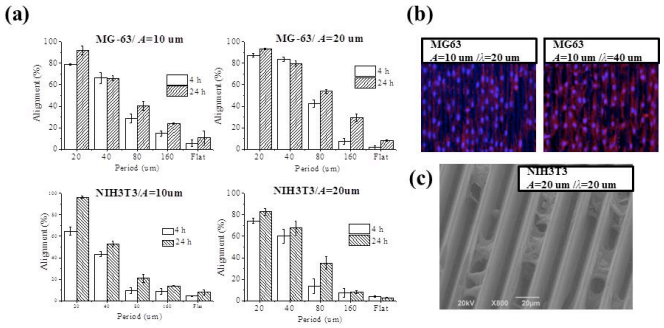

Figure 1. (a) cell alignment data, (b) staining images, and (c) SEM image.

Conclusions

In this study, GPS was designed with the cell size taken into account and manufactured by LIGA to realize the pseudo-3D microenvironment. We investigated the cell alignment in view of two criteria. The cell culture results indicated that the steepness of groove wall and the spatial margin affected the cell alignment. This GPS could be useful in biological and tissue engineering researches.

References

[1] Sanz-Herrera JA et al., Biomaterials. 2009;30:6674-86.
[2] Sukmana I et al., J Biomed Mater Res A. 2010;92A:1587-97.

Acknowledgements

This work was supported by the Industrial Core Technology Development Program funded by the Ministry of Knowledge Economy (No.10041913).

Biofabrication of multi-material anatomically shaped tissue constructs

Jetze Visser[1], Benjamin Peters[1,2], Thijs Burger[1], Jelle Boomstra[3], Wouter Dhert[1,4], Ferry Melchels[1,5], Jos Malda[1,5,6]

1. Department of Orthopaedics, Netherlands Institute of Regenerative Medicine, University Medical Center Utrecht, Utrecht, The Netherlands.
2. University of Denver, Denver, Colorado, USA
3. Protospace, Fablab Utrecht, Utrecht, The Netherlands
4. Faculty of Veterinary Sciences, Utrecht University, Utrecht, The Netherlands
5. Institute of Health and Biomedical Innovation, Queensland University of Technology, Brisbane, Australia
6. Department of Equine Sciences, Faculty of Veterinary Sciences, Utrecht University, Utrecht, The Netherlands

Introduction

Additive manufacturing in the field of regenerative medicine aims to fabricate organized tissue-equivalents[1]. However, the control over shape and composition of biofabricated constructs is still a challenge and needs to be improved. The current research aims to improve shape, by converging a number of biocompatible, quality construction materials into a single three-dimensional fiber deposition process.

Materials and Methods

To demonstrate this, several models of complex anatomically shaped constructs were fabricated by combined deposition of poly(vinyl alcohol), poly(e-caprolactone) (PCL), gelatin methacrylamide (gelMA)/gellan gum and alginate hydrogel. Sacrificial components were co-deposited as temporary support for overhang geometries and were removed after fabrication by immersion in aqueous solutions. Equine chondrocytes were embedded in the gelMA/gellan component in order to evaluate the effect of the fabrication and the sacrificing procedure on cell viability.

Results and Discussion

It was shown that anatomically shaped constructs can be successfully fabricated, yielding advanced porous thermoplastic polymer scaffolds, layered porous hydrogel constructs, as well as reinforced cell-laden hydrogel structures. For example, a miniaturized distal femur was fabricated with two gelMA/gellan components representing the bone and cartilage components, with PCL as a temporary support structure (figure 1). Chondrocytes embedded in these constructs maintained a high viability after the fabrication processes.

Conclusions

In conclusion, anatomically shaped tissue constructs of clinically relevant sizes can be generated when employing multiple building and sacrificial materials in a single biofabrication session. The current techniques offer improved control over both internal and external construct architecture underscoring its potential to generate customized implants for human tissue regeneration.

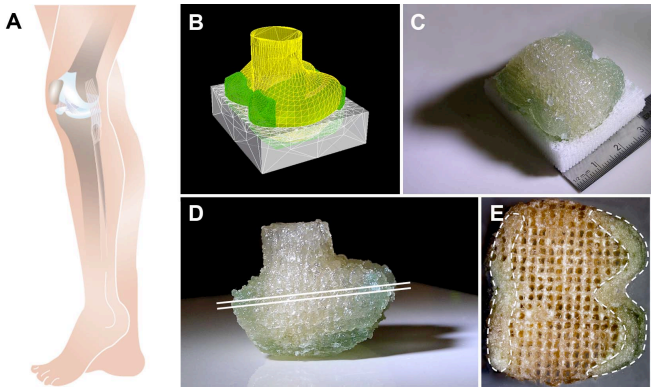

Figure 1.

References

1. Melchels FPW DM, Klein TJ, Malda J, Bartolo PJ, Hutmacher DW. Additive manufacturing of tissues and organs. *Progress in Polymer Science*. 2011;37:1079-1104

Acknowledgements

The research leading to these results has received funding from the European Community's Seventh Framework Programme (FP7/2007-2013) under grant agreements n°309962 (HydroZONES) and n°272286 (PrintCART). Jetze Visser was supported by a grant from the Dutch government to the Netherlands Institute for Regenerative Medicine (NIRM, grant n°FES0908) and Jos Malda was supported by the Dutch Arthritis Foundation.

Bioprinting of 3D Scaffolds with Controlled Architecture for Patient-Specific Auricular Tissue Regeneration

Héctor Martínez-Ávila [a], Manuela Seliger [a], Emelie Arvidsson [b], Eva-Maria Feldmann [c], Johan Sundberg [a], Nicole Rotter [c] and Paul Gatenholm[a]

[a] Biopolymer Technology, Department of Chemical and Biological Engineering, Chalmers University of Technology, Gothenburg, Sweden
[b] Biology Education Centre, Uppsala University, Uppsala, Sweden
[c] Ulm University Medical Center Hospital, Ulm, Germany

Introduction

Bacterial nanocellulose (BNC) is a promising non-resorbable biomaterial for auricular cartilage tissue engineering. This natural polymer, synthesized by the bacterium *Gluconacetobacter xylinus*, is composed of highly hydrated fibrils (99% water) with high mechanical strength. *In vivo* biocompatibility of BNC has been established [1]. Additionally, *in vitro* studies with human ear and nasal septal chondrocytes, fibroblasts and osteoprogenitor cells have shown good cell adhesion, migration and ECM production in BNC scaffolds [2, 3, 4].

This work describes a novel biofabrication method, which uses bacterial machinery and printing technology to engineer BNC scaffolds with features at different length scales – ranging from the nano to the macro and large scales.

Materials and Methods

A 3D Bioprinter (described elsewhere by Nimeskern et al.[5]) was developed in-house for the production of porous BNC scaffolds. Culture medium, with or without porogens, is dispensed with this bioprinting system, were the bacteria use the sugar in the medium to synthesize a porous network of nanosized cellulose fibrils. The nanoscale features of the scaffolds were modified by changing the culture medium composition. The macroscale features were incorporated by dispensing a suspension of calcium-crosslinked alginate porogens (Ø 200-300 μm) during the BNC production. The scaffolds were then harvested for cleaning with 100mM NaOH. The porogens were removed by washing with 50mM sodium citrate, to chelate the calcium and uncrosslink the alginate, and subsequently washing with deionized water. The scaffolds were then sterilized by autoclaving. An *in vitro* study was performed to evaluate the cell migration into the scaffold and the results were evaluated histologically. The morphology of the scaffolds was evaluated with scanning electron microscopy (SEM).

The large scale features were controlled by using a negative ear mold to guide the bacteria to reproduce the auricular shape. Medium was added on-demand for 14 days as the bacteria produced the BNC auricular scaffolds layer by layer. The ear-shaped scaffolds were then washed with 100mM NaOH and deionized water.

Results and Discussion

The results showed that the cellulose production is influenced by the culture medium composition. This in turn affects the mechanical properties of the BNC material.

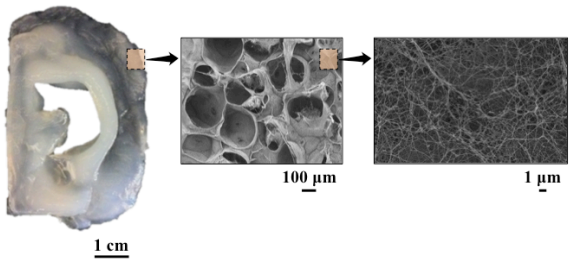

Figure 1. Multiscale BNC auricular scaffold.

With the use of this bioprinter we were able to produce porous BNC scaffolds by introducing alginate porogens during the bacterial culture. The bacteria synthesized the nanocellulose around the packed layers of alginate beads. Macroporous BNC scaffolds were obtained after the removal of the porogens (see figure 1). Nevertheless, the histological evaluation showed a limited cell migration into the scaffolds after 7 days in culture. This is due to the limited interconnectivity between the pores, which depends on the packing density of the alginate beads during the biofabrication process. Furthermore, a patient-specific BNC auricular scaffold was successfully produced with this bioprinter (Fig. 1).

Conclusions

The biofabrication method described here is a true example of bioprinting scaffolds with features at different length scales. Furthermore, different medium compositions were used to produce BNC with varying mechanical properties. In the future, we could use different culture medium simultaneously to synthesize scaffolds with mechanical property gradients, or to increase the stiffness of the scaffold locally.

References

1. Helenius G., et al. (2006). J Biomed Mat Res A.
2. Feldmann EM., et al. (2013). J Biomater Appl.
3. Andersson J., et al. (2010). J Biomed Mat Res A.
4. Martinez H., et al. (2012). J Biomed Mat Res A.
5. Nimeskern L., et al. (2013). J Mech Behav Biomed.

Acknowledgements

The authors acknowledge ERA-NET/EuroNanoMed (EAREG-406340-131009/1) for funding this work.

Direct Bioprinting of Perfusable Vascularized Tissues

Yin Yu and Ibrahim T. Ozbolat
Biomanufacturing Laboratory
The University of Iowa, Iowa City, IA, 52242

Introduction

In order to fabricate three-dimensional tissue constructs, living cells can be delivered from the printer to the printed structure via biomaterial as a transferring medium; however, biomaterial inclusion should be minimized due to degradation-related complications, fewer cell-to-cell interactions in the biomaterial curser, and the long-term side effects of cells waiting in precursor solution in the bioprinter unit [1]. Cell aggregates could be a potential solution to this problem by using spheroids that are manufactured using hanging-drop cultures or micro-patterned molds. Cell aggregates in spheroid form have recently been researched and used in bioprinting of tissues, showing their potential for tissue fusion and quick maturation [2]. Although, spheroid-based aggregate techniques are promising for tissue engineering, their labor-intensive fabrication in limited scale makes their applicability for large-scale tissue/organ fabrication difficult. Moreover, printing them sequentially by ensuring contact between each adjacent spheroid is another hurdle that brings gaps and openings in the tissue [1]. Besides, hydrogels are required as a transferring medium to deposit spheroids. In this work, we propose a novel approach in fabrication of perfusable vascularized tissues using a hybrid bioprinting methodology, where vascular network is integrated with cylindrical cell aggregates. A new practical technique is used to fabricate cell aggregates in cylindrical form for direct printing showing great promise for scale-up tissue fabrication.

Materials and Methods

Human umbilical vein smooth muscle cells in $1x10^7$ /ml concentration were encapsulated in 3-4% sodium alginate solution uniformly and printed through a coaxial nozzle unit, where 0.5% calcium chloride was ejected through the core section for gelation of the vascular conduit leaving an unblocked vasculature [3]. Then, fibroblast cells were used to fabricate cylindrical cell aggregates using a new microfluidics-based approach, which were then printed in tandem with the vasculature using a unique bioprinter, the Multi-Arm BioPrinter (MABP) (Fig. 1A). The MABP provided fabrication of a hybrid construct in a mold to keep the printed construct mechanically integrated until fusion was partially achieved. Then the printed construct was perfused in a custom-made perfusion chamber for the maturation of the tissue. Sample tissues were fabricated and viability, functionality and histology studies were conducted.

Results and Discussion

We fabricated cylindrical cell aggregates with approximately 100% cell viability (data not shown here), where cell aggregates were directly printed in a mold and the vasculature was integrated during hybrid printing process. Figure 1B shows a vasculature printed separately, where viability of smooth muscle cells increased during the first week and reached 85.5±0.1% under perfusion. Reasonable elastin deposition was obtained during 2 months in-vitro culture. We used the vasculature during hybrid fabrication approach (Fig. 1C), where continuous cell aggregates were printed and integrated around the vasculature. After five days, fusion of fibroblast aggregates resulted in a tubular tissue surrounding smooth muscle vasculature (Fig. 1D). Figure 1E demonstrates the cross-section, where cylindrical cell aggregates fused and enclosed the vasculature tightly, and were contracted around the vasculature.

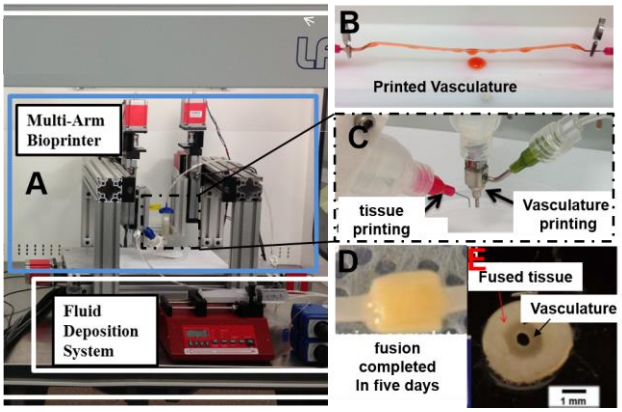

Figure 1. (A) The MABP, (B) a printed vasculature in a perfusion chamber, (C) the MABP enables tandem printing of the vasculature and the tissue using dual independent printer units, (D) cell aggregates fused and enclosed the vasculature after five days post-printing, (E) where sectioning shows gap-free perfect fusion.

Conclusions

In this research, a new hybrid approach is demonstrated for fabrication of perfusable vascularized tissues, which is highly promising for scale-up fabrication technology for various tissues and organs. In addition to fibroblast cells, we also experimented cartilage progenitor cells and beta TC3 cells. We will further develop scale-up tissue models with complex vascular network using the MABP with a fully-automated process.

References

[1] Ozbolat, I. T., and Yu, Y., 2013, "Bioprinting Towards Organ Fabrication: Challenges and Future Trends," IEEE Trans. Biomed. Eng., 60(3), 1–9.
[2] Mironov, V. et al., 2009, "Organ printing: Tissue spheroids as building blocks", Biomaterials, 30, 2164-74.
[3] Zhang, Y. et al, 2013," Characterization of Printable Cellular Micro-Fluidic Channels for Tissue Engineering," Biofabrication, 5(2), p. 024004.

Acknowledgements

This research has been supported by the National Institutes of Health (NIH) and the Institute for Clinical and Translational Science (ICTS) Grant No. ULIRR024979.

In vivo and *in situ* bioprinting of cells and biomaterials to guide tissue repair

Virginie KERIQUEL[1], Sylvain CATROS[1], Sophia ZIANE[1], Reine BAREILLE[1], Murielle RÉMY [1], Samantha DELMOND[2], Benoit ROUSSEAU[3], Joëlle AMÉDÉE[1], Fabien GUILLEMOT[1] and Jean-Christophe FRICAIN[1]

[1] Inserm U1026, Université Bordeaux Segalen, Bordeaux Cedex 33076, France,
[2] CHU Bordeaux, CIC-IT, 33300 Pessac, France,
[3] Univ. Bordeaux, Animalerie A2, 33000 Bordeaux, France

Introduction

The development of Computer-Assisted Medical Interventions (CAMI) results from converging evolutions in medicine, physics, materials, electronics, informatics and robotics. CAMI aim at providing tools that allow the clinician to use multi-modal data in a rational and quantitative way in order to plan, simulate and execute mini-invasive medical interventions accurately and safely. In parallel, technological advances in the fields of automation, miniaturization and computer aided design and machining have also led to the development of bioprinting technologies which could be defined as the computer-aided, layer-by-layer deposition, transfer and patterning of biologically relevant materials.

Materials and Methods

In this paper, we present the first demonstration of bioprinting 3D tissue constructs *in situ* and *in vivo*. These constructs were realized by depositing sequentially a collagen solution (type I) and mouse mesenchymal stem cells (from D1 cell line) that were realized using Laser-Assisted Bioprinting into critical size mouse calvaria defects. The MSC patterns were initially observed using intravital microscopy and D1 cells previously infected with lentivirus expressing the red fluorescent protein tdTomato. Cell proliferation was also followed-up till 8 weeks by measuring bioluminescence from D1 cells previously infected with a luciferase-expressing lentivirus using photon–imager (Biospace). Histological analysis of printed tissues was done at different time points using decalcified sections and X-ray microtomography.

Results

Laser-assisted Bioprinting allows to deposit patterns of cells *in situ* and *in vivo* (Fig.1) at a cell-level resolution. D1 cells printed *in vivo* survive, migrate and the results show a proliferation *in vivo for* 35 days. Moreover, histological analyses of the decalcified samples observed after 5 weeks of healing revealed presence of newly formed trabecular of woven bone (Fig.2).

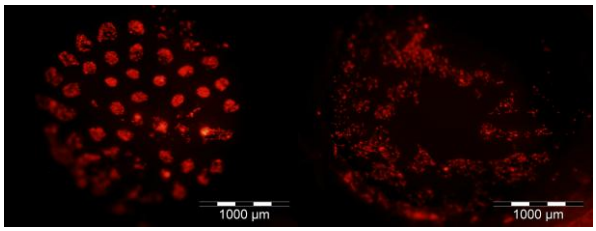

a b

Fig.1. Fluorescent image of D1-td-Tomato cells printed *in situ* (calvaria) with two patterns. (a) 2mm diameter-disk and (b) ring with 2.4/1.3mm external and internal diameters.

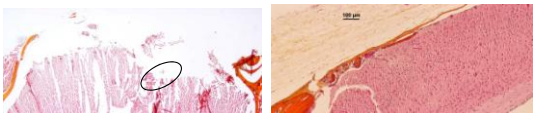

a b

Fig 2. Histological pictures (HES staining) of materials implanted in the calvaria defects after 5 weeks. (a) Frontal section of the calvaria implanted with collagen and D1td-Tomato cells (disk) (x2). (b) High magnification of site implanted with collagen and D1Td-tomato cells (ring) (X10).

Discussion and Conclusions

In conclusion, these results pave the way of using bioprinting technologies for Computer-Assisted Medical Interventions. More precisely, we show that 3D tissue constructs can be printed *in vivo* and *in situ* in relation with defect morphology. Interestingly, we demonstrate that printing cells *in situ* with a cell-level resolution tends to orientate tissue repair.

References

1. Keriquel V and al. Biofabrication **2**, 014101, 2010.

Acknowledgments

The authors would like to thank the “Région Aquitaine”, “the Institut Français de la Recherche Médicale (IFRO)” and the “Agence Nationale de la Recherche (ANR)” for their financial support.

Disclosures

The authors have no financial affiliation that would have biased this article.

Fabrication of Three-Dimensional Tubular Constructs using DOD Inkjetting

Changxue Xu[1], Yong Huang[2]
[1]Clemson University, Department of Mechanical Engineering, Clemson, SC 29634, USA, changxx@clemson.edu
[2]University of Florida, Department of Mechanical and Aerospace Engineering, Gainesville, FL 32611, USA, yongh@ufl.edu
Oral and Poster

Introduction

Organ printing offers a great potential for the fabrication of three-dimensional (3D) living tissues and organs by precisely layer-by-layer placing various tissue spheroids spatially [1-3]. The fabricated tissues and organs can be used for the replacement of damaged or injured human organs, leading to a promising solution to the challenge of organ donor shortage. Of different biofabrication methods, inkjet printing is a promising bioprinting technique because it can be scaled up to dispense biological fluids as needed, eliminate waste and allow a good spatial printing resolution. There are two forms of inkjet printing, continuous inkjet (CIJ) printing and drop-on-demand (DOD) printing. During CIJ printing, a liquid is ejected from a small orifice to form a jet which spontaneously breaks up into a stream of droplets due to the Rayleigh instability. During DOD printing, droplets are generated only when required, by propagating a pressure pulse in a fluid filled chamber. DOD printing was favored here due to its good controllability and less contamination. In this study, 3D tubular constructs with or without cells inside were fabricated vertically and horizontally without support materials.

Materials and Methods

Sodium alginate (Sigma-Aldrich, St. Louis, MO) was used to make 1% (w/v) sodium alginate bioink for vasculature-like construct fabrication by mixing it with NIH 3T3 mouse fibroblast suspension. The cross-linking solution was 2% (w/v) calcium chloride (Sigma-Aldrich, St. Louis, MO).

The platform-assisted inkjet 3D printing system used in this study had three key parts: motorized XY stages attached with a computer-controlled nozzle dispenser, a motorized Z stage attached with a Z-shape platform where constructs were printed, and a container containing the cross-linking solution. The XY stages were precisely controlled to define the dispense head location for planar feature printing, and the Z stage was controlled moving down vertically to match the printing speed for each deposited layer. Under the vertical printing configuration, the dispense nozzle moved along the circumferential direction of tube during fabrication while under the horizontal printing configuration, the dispense nozzle moved parallel to the tube longitudinal axes during the fabrication of each layer.

Results and Discussion

Vasculature-like tubular constructs with an overhang have been successfully fabricated by sequentially depositing sodium alginate-based bioink into calcium chloride solution using both vertical printing and horizontal printing. Some representative results are shown in Figures 1 and 2.

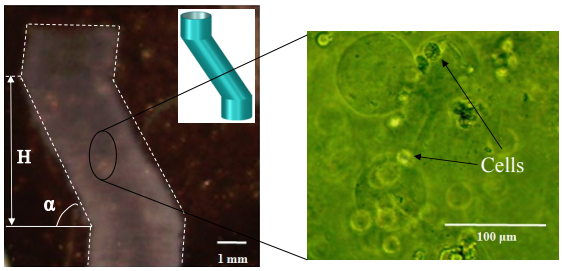

(a) (b)

Figure 1. (a) Cellular tubular construct fabricated using vertical printing and (b) some embeded cells

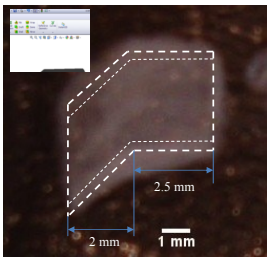

Figure 2. Tubular construct fabricated using horizontal printing

Conclusions

Both the vertical and horizontal inkjet printing configurations are capable of making tubular constructs with an overhang. It is envisioned that truly 3D vascular constructs such as a vascular tree should be fabricated using the combination of vertical and horizontal printing.

References

[1] Nakamura, M., Kobayashi, A., Takagi, F., Watanabe, A., Hiruma, Y., Ohuchi, K., Iwasaki, Y., Horie, M., Morita, I., and Takatani, S., 2005, "Biocompatible inkjet printing technique for designed seeding of individual living cells," Tissue Engineering, Vol. 11, pp. 1658-1666.

[2] Boland, T., Tao, X., Damon, B.J., Manley, B., Kesari, P., Jalota, S., and Bhaduri, S., 2007, "Drop-on-demand printing of cells and materials for designer tissue constructs", Materials Science and Engineering: C, Vol. 27, pp. 372-376.

[3] Xu, C., Chai, W., Huang, Y., and Markwald, R.R., 2012, "Scaffold-free inkjet printing of three-dimensional zigzag cellular tubes," Biotechnology and Bioengineering, Vol. 109, pp. 3152-3160.

Acknowledgements

The work was partial supported by the National Science Foundation (NSF EPS-0903795 and CMMI-1100402).

Novel biofabricated devices enabling *in vitro* and *in vivo* screening in 3D.

Carlos Mota, Gustavo A. Higuera, Joost van Dalum, Clemens van Blitterswijk, and Lorenzo Moroni
Department of Tissue Regeneration, University of Twente, Drienerlolaan 5, 7522NB Enschede, The Netherlands. Tel: +31534893502; Fax: +31534892150; E-mail: l.moroni@utwente.nl.
Preferred format: Oral.

Introduction

In all biomedical fields, new treatments, therapies, or agents relevant for the improvement of health care need to be tested in animal models before reaching the clinics. Although a lot of effort is being placed on finding suitable *in vitro* model systems to replace *in vivo* testing, currently developed solutions fail to recapitulate biological complexity. Therefore, *in vivo* experiments are still necessary. Enabling technology allowing reduction of experimental animals would impact tremendously the associated costs and ethical issues. In this study, we have explored an alternative route that can potentially abate the number of lives and expenses in animal testing through the development of implantable three-dimensional (3D) screening systems. We show how these devices can be used to find improved therapies in the field of regenerative medicine and hold potential as drug discovery platform for cancer.

Materials and Methods

Free-form fabrication and biomaterials furnish the versatility necessary to design and produce wells of size organized in column × row arrays (Macroarrays). Bioplotter and stereolithography (Envisiontec) were used to make the well macroarrays with a fabrication process adapted from that for scaffold fabrication (1).

To test the macroarray devices for regenerative medicine applications, a total of 36 extracellular matrix (ECM)-producing experimental conditions comprising various cell numbers of human mesenchymal stem cells (hMSCs), primary bovine chondrocytes and cocultures of these two cell types were dispensed in separate wells of macroarrays, implanted in one immunodeficient mouse (n=10 mice), examined through histological sections and screened for cartilage through glucosaminoglycans.

To test the potential of these devices for cancer applications, human osteosarcoma (MG-63) and human colon adenocarcinoma (SW480) cell lines were seeded *in vitro* in each well at different cell densities in the presence of known chemotherapeutic agents (e.g. 5- fluorouracil) at different drug concentrations . Cell viability was assessed through live/dead and DNA assays.

Results and Discussion

Depending on the size of the animal, these platforms can be tailored to fit the required dimensions of an implantation site, which defines the number of conditions that can be implanted. Thus, the bigger the animal, the higher the number of conditions that can be investigated simultaneously (Figure 1) in macroarrays made of different polymers. With the flexibility offered by rapid prototyping, macrorrays can have wells varying in size and architectures from μm^3 to mm^3.

hMSCs, chondrocytes and co-cultures thereof were successfully seeded *in vitro* and resulted in a variable degree of tissue regeneration *in vivo*. Specifically, the higher the hMSCs concentration the higher was the tissue formed in the wells, with a 4:1 hMSCs:chondrocyte ratio being the best in cartilage tissue formation.

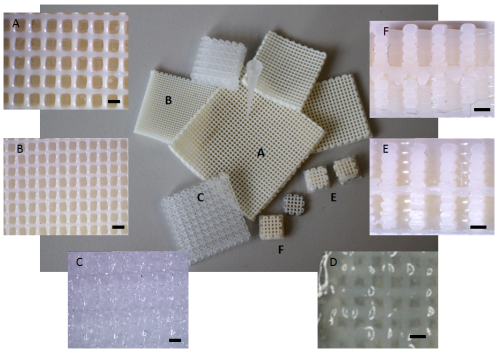

Figure 1. Macroarrays with different dimensions can be fabricated: 1024 wells (A) and 100 wells made of PEOT/PBT (B); 100 wells made of of poly lactic acid (C); 100 wells made of alginate (in PBS) (D). Different architectures could also be created: double matrix (top and bottom of a system) with a solid polymer layer in between (E); wells with a porous layer of material in the middle to enable co-culture (F). Scale bar: 1 mm.

Preliminary *in vitro* studies for cancer therapy showed that these devices hold the potential to be used also as platform to screen the effect of drugs on cells in 3D, which has been recently shown to be a more reliable method to discover new therapies (2). Initial experiments seem to indicate a higher cell death with increasing the concentration of known chemotherapeutic agents. Further studies will aim at confirming these data both *in vitro* and *in vivo*.

Conclusions

With the previously described macroarray devices the use of vertebrate animal lives and costs could be drastically dwindled in pharmaceutical, toxicological, chemical, and disease screening.

References

1 L. Moroni, J. R. de Wijn, C. A. van Blitterswijk, *Biomaterials* **27**, 974 (Oct, 2006).

2. V.S. Nirmalanandhan, A. Duren, P. Hendricks, G. Vielhauer, G.S. Sittampalam. *Assay Drug Dev Techn* **8**, 581 (May 2010).

Acknowledgements

This work is financially supported by grant number 93611002 of the Netherlands Genomics Initiative.

Toward complex tissues engineering: Study of self-organization processes using Laser-Assisted Bioprinting

E. Pagès[1], M. Medina[1], M. Rémy[1], B. Guillotin[1], R. Devillard[1], F. Guillemot[1]
[1] *Inserm U1026, Université Bordeaux Segalen - BioTis, Bordeaux Cedex 33076, France*

Introduction

Laser-Assisted Bioprinting (LAB) is an emerging technology in tissue engineering. It allows to print cells and liquid materials with a controlled cell density and microscale organization [1]. By controlling the cell 3D microenvironment using LAB, we hypothesize that morphogenetic processes might occur and lead to the fabrication of complex living tissues. In this context, our work aims at evaluating the influence of stem cells spatial patterning on self-organization processes.

Materials and Methods

Cells used in these experiments are human and mouse mesenchymal stem cells. Bio-inks are made up with cells suspended into culture medium. The bio-paper is a collagen type I hydrogel layer. Printing parameters are controlled to tune cell pattern features: localization of each cell islet on the bio-paper and number of cells per islet. Cell viability, adhesion, proliferation and differentiation are evaluated after the LAB process. Time lapse video microscopy is used to follow cell migration. Data are analyzed using Image J and the Chemotaxis Tool Plug-in.

Results and Discussion

After LAB, cell viability is maintained; cells are able to adhere to collagen and to differentiate (Fig.1). A proportional rate of proliferation is measured for printed and non printed cells.

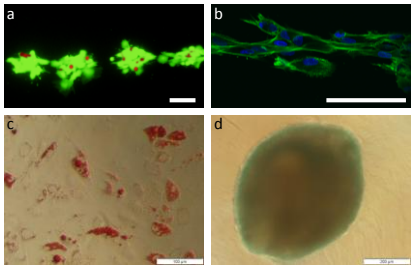

Figure 1. Observation of cell viability (a), cell spreading (b), adipocyte and chondrocyte cell differentiation (resp. c and d) after bioprinting. Scale bar: 100µm

The printing pattern is parallel lines of cell islets. For a distance of 250 µm between 2 cell islets, cell migration occurs and a continuous line is formed at 24 h. When this islet-to-islet distance is larger than 250 µm, cells keep isolated till 72 h (Fig. 2).

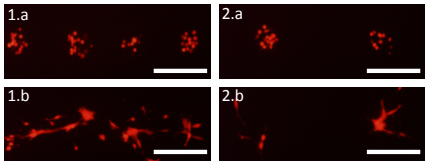

Figure 2. Initial islet-to-islet distances (250 (1) and 500 µm (2)) influence cell self-organization at 1 (a) and 72 h (b). Scale bar: 200µm

When this distance equals 250 µm, and the number of cells per islet is about 10, thin and continuous cell fibres are observed after 24 h. These fibres remain stable till 72 h but can be disturbed when other lines of cell are closer than 1000 µm. Interestingly, by reducing the islet-to-islet distance in both directions to 250 µm, cells form a homogeneous layer at 48 h (Fig. 3).

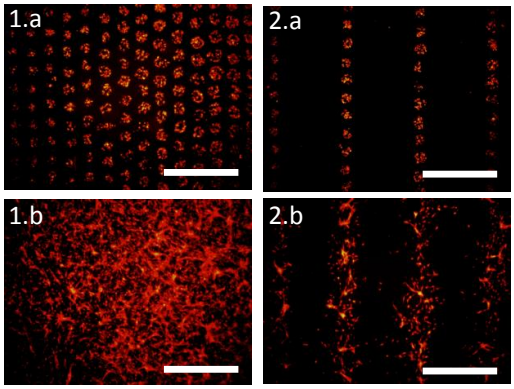

Figure 3: Distance between cell lines (250 (1) and 1000 µm (2)) induces formation of specific cell patterns at 1h (a) and 48h (b). Scale bar: 1000µm

Cell migration is studied more thoroughly for a pattern of 250 µm between islets within a line and 1000µm between lines. Pictures are taken every 15 minutes during 45 hours after printing. Quantitative analysis of cell migration through center of mass movements reveals that within the cell pattern there is directed cell migration in 3 stages. First cells of an islet tend to cluster; then cells of islets distant of 250 µm migrate from one to another to form continuous cell fibres; during the third stage cells start to migrate from one line to another.

Conclusions

The ability to position cells at cell level resolution using LAB allows studying their migration in different conditions (e.g. microenvironment). Results demonstrate that by controlling the initial cell pattern, it is possible to obtain distinct cell organization.

References

[1] Guillotin, B., et al. (2010). Laser assisted bioprinting of engineered tissue with high cell density and microscale organization. Biomaterials , Volume 31, Issue 28, Pages 7250–7256.

Acknowledgements

ANR and Region Aquitaine for financial support.

Indirect three-dimensional printing of a tracheal bellows graft

Jeong Hun Park[1], Ju Young Park[2], In-Chul Nam[3], Sung Won Kim[4], Young Hoon Joo[5], Hyun-Wook Kang[6], and Dong-Woo Cho[1] *

[1]Department of Mechanical Engineering, POSTECH, Pohang, Gyeongbuk, Korea
[2]Division of Integrative Biosciences and Biotechnology, POSTECH, Pohang, Gyeongbuk, Korea
[3]Department of Otolaryngology-HNS, College of Medicine, The Catholic University of Korea, Incheon, South Korea
[4]Department of Otolaryngology-HNS, College of Medicine, The Cartholic University of Korea, Seoul, South Korea
[5]Department of Otolaryngology-HNS, College of Medicine, The Cartholic University of Korea, Bucheon, Korea
[6]Wake Forest Institute for Regenerative Medicine, Wake Forest University, Medical Center Boulevard, Winston-Salem, NC27157, USA
* Corresponding author: dwcho@postech.ac.kr

Introduction

Several artificial tracheal grafts for tracheal reconstruction involving tracheal epithelial regeneration have been introduced through tissue engineering. However, none has considered actual structural and mechanical properties of the native trachea.

Herein, a novel composite tracheal graft consisted of a bellows scaffold and a none-degradable ring structure was developed for mimicking the structure and mechanical behavior of the native trachea. Monolayered sheet of Human turbinate mesenchymal stem cells (hTMSCs) was also applied to hasten tracheal epithelial regeneration. Developed tracheal graft had similar mechanical behavior to rabbit's native trachea and its epithelial regeneration ability by hTMSC sheet was also validated by in vivo test using rabbit model

Materials and Methods

A bellows scaffold was designed on the basis of the morphology of rabbit's native trachea and it was fabricated using indirect three-dimensional printing (3DP) technique. A Sacrificial mold having negative shape of the bellows scaffold was first fabricated using projection-based micro-stereolithography (pMSTL), one of the 3DP techniques, with alkali-soluble photopolymer. Then, the PLCL solution (150%, w/v) and gelatin solution (80%, w/v) were mixed and then injected into the mold. The mold was immersed in isopropyl alcohol (IPA) and glutaraldehyde solution sequentially for PLCL hardening and gelatin cross-linking, respectively. The sacrificial mold was finally dissolved in NaOH to obtain the bellows scaffold. Meanwhile, the non-degradable ring structure was fabricated using biomedical grade silicone rubber and assembled to the outer grooves of the bellows scaffold.

After fabricating a tracheal graft, cultured hTMSCs monolayer was attached on the inner surface of a tracheal graft for 3 days. The hTMSCs sheet-attached tracheal graft was then implanted into the non-circumferential tracheal defect and tracheal epithelial regeneration was evaluated after 4 weeks.

Results and Discussion

A novel composite tracheal graft was successfully fabricated. The mechanical behavior of fabricated bellows graft was compared with rabbit's native trachea in terms of three-point bending and radical compression. In the result of three-point bending test, two structures have almost same load values for 1mm displacement. The load of tracheal graft was higher than that of native trachea over the whole displacement range for radial compression. Therefore, bellows tracheal graft has higher mechanical strength to keep the lumen open under radial compression than that of rabbit's native trachea.

In vivo results, hTMSCs sheet attached bellows graft showed complete ciliated columnar epithelium in the luminal surface of the tracheal graft after 4 weeks. Epithelial cells were also arranged well and basal cells formed thick basement.

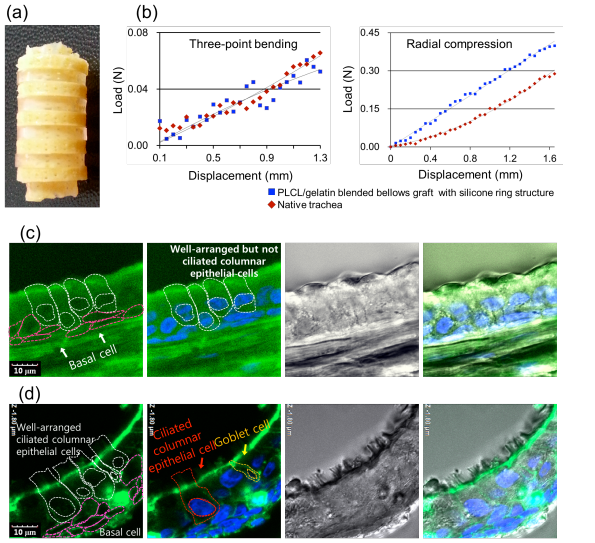

Figure 1. Development of bellows tracheal graft and in vivo results. (a) PLCL/gelatin blended bellows graft assembled with silicone ring structure. (b) Load and displacement curve for three-point bending (left) and radial compression (right). Morphological analysis of regenerated tracheal epithelium of in vivo (c) without hTMSCs sheet and (d) with hTMSCs sheet.

Conclusions

In conclusion, bellows tracheal graft was successfully developed. Developed tracheal graft with hTMSCs sheet will be a promising alternative for tracheal reconstruction with good mechanical behavior.

Acknowledgements

This work was supported by the National Research Foundation of Korea (NRF) grant funded by the Korea government (MSIP) (No. 2010-0018294).

Bioprinting of Human Pluripotent Stem Cells for Liver Tissue Generation

Alan Faulkner-Jones[1], Catherine Fyfe[2], Jason King[2], John Gardner[2], Aidan Courtney[2], Wenmiao Shu[1]*

[1]Institute of Biological Chemistry, Biophysics and Bioengineering, Heriot-Watt University, Edinburgh, UK

[2]Roslin Cellab, Roslin Biocentre, Midlothian, UK

ajf10@hw.ac.uk, *w.shu@hw.ac.uk

Introduction

The ability to create precise in vitro cultures of cells is essential for replicating the *in vivo* microenvironment. A number of studies have shown that certain cells require a three-dimensional structure in order to function properly. Therefore, if more complex structures such as those found in organs were to be printed, the bioprinter would need the ability to transfer mesoscopic patterns of viable cells into well-defined three-dimensional arrays. This project develops innovative valve-based bioprinters that have been validated to print highly viable cells with independent control of the position and volume of each droplet. Droplets can be made from up to four different bio-inks and the proportion of each bio-ink is controllable. The 3D bioprinting of human pluripotent stem cells with hydrogel materials is attempted to regenerate human liver tissue for animal-free drug testing applications.

Materials and Methods

Using our previously reported Bioprinter, we performed a more detailed investigation into the response of human stem cells to the valve-based printing process. To evaluate the cellular viability post printing, stem cells were stained with either propidium iodide (PI) and processed using fluorescence-activated cell sorting (FACS) or 4'-6-Diamidino-2-phenylindole (DAPI) fluorescent dye and observed under a fluorescent microscope.

In order to confirm the stem cells were still pluripotent, multiple samples of printed cells were fixed 5 days post-printing before primary and then secondary antibodies for selected pluripotency/differentiation markers were added to the fixed cells. OCT4, SSEA1, NANOG and SOX2 markers were tested for on two hESC lines (RC6 and RC10). Samples were analysed on a fluorescent microscope or a FACS machine.

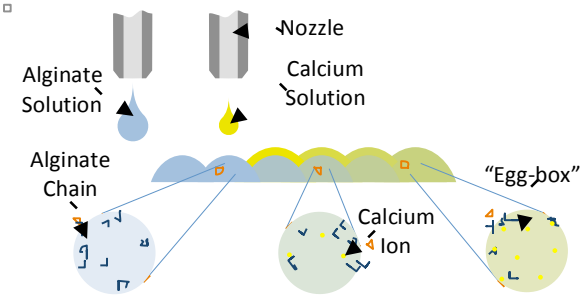

Figure 1. Schematic of the hydrogel printing process

hESCs were directed to differentiate into hepatocyte-like cells (HLCs) using a modified Hay protocol. These cells were then printed into a 3D hydrogel matrix (Figure 1) and cultured by adding medium to the hydrogel matrix and incubating. The resulting micro-tissue structures were used to verify that the differentiation proceeded normally.

Results and Discussion

The printed hESCs were shown to retain cellular viability and pluripotency post printing.

Several test patterns were printed out using different concentrations of alginate hydrogel (e.g. 0.1%-3%) with the smallest feature size of ~337 µm achieved. Patterns included simple lines with several layers stacked vertically (Figure 2 left) and octagons measuring 3 mm in diameter (Figure 2 right).

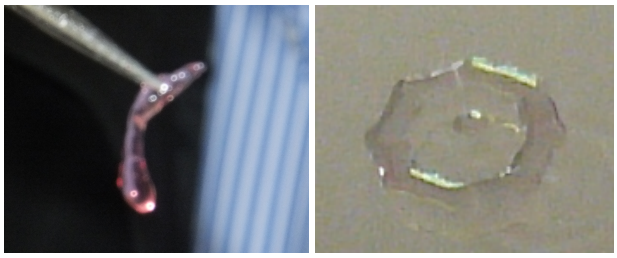

Figure 2. Printed hydrogel structures

hESCs (RC10) were successfully induced to differentiate into HLCs (Figure 3) after 20 days.

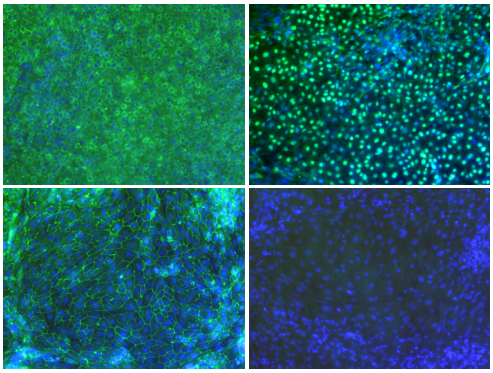

Figure 3. Day 17 HLCs from modified Hay protocol

Conclusions

This study shows that the 3D Bioprinting technique is compatible with stem cell transfer as the dispensed cells were found to be highly viable and remained pluripotent. Furthermore, the properties and geometry of the 3D hydrogel matrix can be varied to generate 3D structures with well-defined geometry, size and composition.

Further studies will be mainly focused the evaluation of 3D printed HLC tissues for use in drug testing.

Acknowledgements

The authors acknowledge the funding support from the Scottish Universities Physics Alliance (SUPA)'s INSPIRE scholarship sponsored by the Scottish Funding Council.

Generation of Hydrogel Matrixes with a 3D Gradient of Mechanical Properties in a novel 3D Concentration Gradient Bioreactor

G. Orsi[1,2], C. De Maria[1,3], G. Vozzi[1,3]

Introduction

The need to study cells and tissues in environments more similar to physiological ones turns out to be nowadays one of the greatest tools for the development of new biomolecules, and to understand better most of the physiological phenomena at cell and tissue level. Soluble species spatial gradients are known for their morphogenic action during cell development, and they take place in a 3D environment[1]. Moreover the 3D gradient of mechanical properties of each tissue influences cell migration, differentiation and activities. In this work we describe the design and realization of a bioreactor able to generate three-dimensional concentration gradients, and the realization of a gel matrix with a 3D gradient of mechanical properties[2]. The topology of this device has been initially designed and modelled using Computational Fluid Dynamics, and subsequently realized through rapid prototyping techniques. An hydrogel matrix was then polymerized in the main chamber in order to "froze" the gradient. The matrix had an inner gradient of mechanical properties , because a 3D gradient of crosslinker was established in the main chamber before the start of polymerization.

CFD and Modeling

The design of 3D gradient maker generator is started with a CFD analysis. Its performances were evaluated by solving the following set of equations:

$$\rho(\mathbf{u}\cdot\nabla)\mathbf{u} = \nabla\cdot\left[-p\mathbf{I}+\eta\left(\nabla\mathbf{u}+(\nabla\mathbf{u})^{T}\right)\right]$$

$$\nabla\cdot(-D\nabla C) = -\mathbf{u}\cdot\nabla C$$

$$\nabla\cdot\mathbf{u} = 0$$

The gradient bioreactor is composed of a cubic chamber at the centre of the device (2.4 cm side), in which there are the inputs of 4 mixing network perpendicularly placed. The output of the system is placed on the bottom of x-y plane. The mixing structure had 8 inputs and 16 outlets, which are inputs of bioreactor chamber. The bioreactor chamber had only one output. The height of the mixing channels was set to 300 microns. Tetrahedral mesh was used with average size of 0.05 mm in the inlets and 0.5 mm in the mixing chamber. The mixing network design was taken from a previous work [3,4].

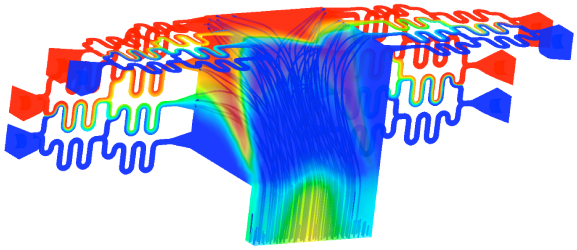

Figure 1: CFD simulation of concentration distribution and streamlines in the gradient maker.

Realization

The mould and the frame of the bioreactor have been made in Acrylonitrile Butadiene Styrene (ABS) using a rapid prototyping system (Dimensione Elite Stratasys®, U.S.A.). The main core has been made casting PDMS (Sylgard 184) in the previous mould. To ensure a perfect sealing a purposely developed locking system (Figure 3) has been designed and realized. It was composed of a plastic frame made of ABS and two Plexiglas layers, in order to maintain a free visual path onto what happened inside the chamber and the microchannels. To ensure a tight sealing of all parts 8 plastic O-rings have been placed between the cylindrical inserts present on the external surfaces of the frame. The deformability of PDMS granted a tight sealing after compression. Figure 4 shows the assembled reactor with the concentration gradient formation inside. Figure 5 also shows different concentration patterns that could be obtained in the GM. A set of peristaltic pumps were used for system perfusion.

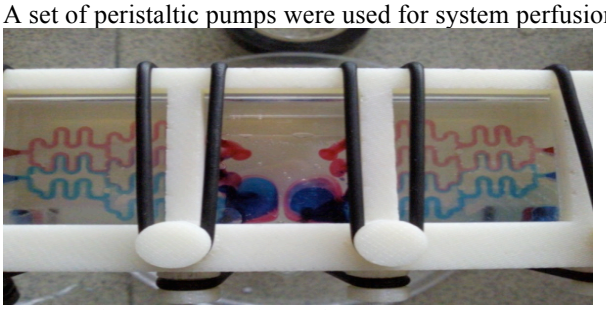

Figure 2: Dye gradient formation into the main chamber of the bioreactor, top view.

Realization of an Hydrogel with a 3D Gradient of Mechanical Properties

Polyacrylamide (PAAM) was chosen as a template hydrogel, due to the easiness in tuning its mechanical properties by just changing the acrylamide (AAM) to bisacrylamide (BIS) ratio (monomer to crosslinker ratio). An 8% w/v solution of AAM with respectively 0.04% w/v or 0.6% w/v of BIS flowed from the inlets, so that a BIS concentration gradient was set in the main chamber. Also the initiator (Amonium Persulfate, AP) was perfused from the inlets. When the steady state was reached an injection of TEMED (catalyst) from a hole in the main chamber quickly polymerized the hydrogel into the main chamber,The 3D controlled distribution of BIS into the gradient chamber lead into the development of a gradient of mechanical properties into the polymerized hydrogel. Reaction time (first gelification in minutes) is significantly higher than BIS diffusion time (several. hours), so we can reasonably be sure that the distribution of BIS remains the same as the applied gradient, even during the polymerization.

Mechanical Testing

The main "cube" was cut in 3 x 3 x 4 small samples, in order to have a good estimation of the distribution of the mechanical properties in the 3D environment. The "cube" was cut using the tools depicted in figure 4, in order to assure an uniform and repeatable slicing. Briefly it was put in the bigger mould, then cut into four slices with an histological sharp blade. Each one of the four slices were then placed in the second mould and then sliced in 9 equal pieces. The choice of critical size was due to the detection limit of our load cell. Each sample was subjected to a compression test using a Zwick-Roell Z005. The Young modulus of the tested sample was evaluated as the slope of first linear part of the Stress-Strain diagram.

Figure 3: PAAM "Cube" with a 3D gradient of mechanical properties resulting from the polymerization of the AAM/BIS filled chamber.

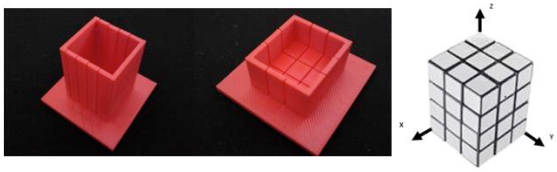

Figure 4: Tools used for "cube" slicing. On the right is shown the "coordinate" system used for samples classification during slicing.

Results

The results of the mechanical testing are shown in figure 5. As it is possible to see there is a gradient of mechanical properties developed in 3D. There is a decrease in Young Modulus from z=1 to z=4, and from y=1 to y=3, following the 3D concentration pattern of the flow.

Conclusion

We have presented a novel class of bioreactor able to generate hydrogel matrices with a 3D gradient of stiffness. This bioreactor could also be used for perfusion of 3D cell scaffolds with a repeatable and stable gradient of chemical species, i.e. growth factor to induce cell differentiation directly into the scaffold.

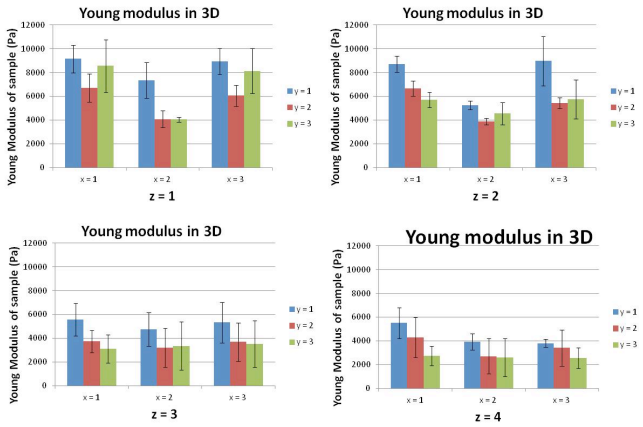

Figure 5: Young modulus measured in gradient samples versus coordinates. It is possible to see a stiffness gradient in z and y directions.

References

1. Engler, A. J., Sen, S., Sweeney, H. L. & Discher, D. E. Matrix elasticity directs stem cell lineage specification. *Cell* **126,** 677–89 (2006).

2. Orsi, G., Carta, V. & Vozzi, G. in *Hydrogels: Synthesis, Characterization and Applications* (NovaPublishers, 2012).

3. Tirella, A., Marano, M., Vozzi, F. & Ahluwalia, A. A microfluidic gradient maker for toxicity testing of bupivacaine and lidocaine. *Toxicology in Vitro* **22,** 1957–64 (2008).

4. Vozzi, G., Mazzei, D., Tirella, A., Vozzi, F. & Ahluwalia, A. Finite element modelling and design of a concentration gradient generating bioreactor: application to biological pattern formation and toxicology. *Toxicology in vitro : an international journal published in association with BIBRA* **24,** 1828–37 (2010).

Collagen-Fibrin Skin graft Using Inkjet Printing Technology: In vivo Testing on an Athymic Nude Mouse Model

Maria Yanez, Aracely Dones, Raoul Gonzales, and Thomas Boland

Introduction

Diabetic foot ulcers and venous leg ulcers are common problems in patients who suffer diabetes type 2. These types of injuries can cause pain, nerve damage, gangrene, and leg amputation reducing the quality of life of people. Due to the inability of diabetic people to heal these type of injuries, they become very difficult to treat, require repetitive treatments and may take months even years to heal. Skin grafting has been used trying to improve wound healing. The majority of grafts are allogeneic and they do not survive several days when are implanted. Recognizing this, we have been studying the behavior of fibroblasts and keratinocytes in engineered capillary-like endothelial networks when embed in a collagen-fibrin matrix. A dermo-epidermal graft has been implanted in athymic nude mouse model to assess the integration with the host tissue as well as the wound healing process.

Materials and Methods

To build the bilayer printed skin graft, a modified inkjet printer was used. This printer allows to customize the shape and create micro-channels where human microvascular endothelial cells (HMVEC) allowing the micro-vascular formation. The main materials of the bilayer skin graft are the fibrin gel and bovine collagen type I. Neonatal human dermal fibroblast cells (NHDF) and neonatal human epidermal keratinocytes (NHEK) are manually mixed in the collagen matrix while HMVECs are dispersed in a thrombin solution and printed at the top of a fibrinogen layer forming the fibrin gel. A full thickness wound was created at the top of the back of the athymic nude mouse and the area was covered by the bilayer skin graft. The mouse was followed until completion of the specified experimental time line, at which time the animals were humanely euthanized, photographed and tissue samples were collected. The tissue was fixed in 10% buffer formalin, and processed for histological and immunohestochemical analysis. The colected pictures were used to assess wound contraction.

Results and Discussion

The mice with printed skin grafts completely healed between 14-16 days. The percentages of wound contraction with respect to the wound on day 0, in the group with the printed skin graft were 69±4%, 71±2.4%, 66±9%, 68±4.4%, and 62.5±9 % at week 2, 3, 4, 5, and 6 respectively. Wound contraction of the printed skin group was improve up to 12% when compare with the commercial available skin graft and the control group. Paraffin sections of the collected tissue have shown epidermal and dermal layer in the testing group, the control group has shown scar tissue formation en the dermal layer and the commercial available group has shown hypergranulation may due to the inflammation response. The paraffin sections stained with H&E have shown evidence of new blood vessel formation in the new skin when the wound bed was covered by the printed skin graft. Immunofluorescence analysis revealed the presence of human cells in the new skin up to 6 week (cell number decreasing over the time) which means that the human cells migrate to the host tissue and help to improve the wound healing process.

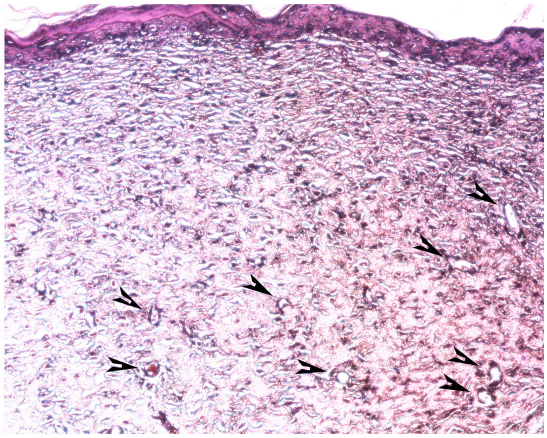

Figure 1. 10X micrograph taken at week 2 after the printed skin graft was applied. Black arrows indicate the small micro channels found in the new skin

Conclusions

The printed skin graft was shown to accelerate the wound healing when it is compared with a commercial available skin wound dressing, and without any type of dressing. The transplantation of printed skin graft transfers part of the artificial in vitro cultivation to the wound area allowing the wound healing. Wound contraction was improved when compared with the other two groups. Histological analysis showed the neoskin, which is closely related to the normal skin. Immunofluorescence studies showed the presence of human cells at the fourth week post-surgery.

References

1. Bello YM, Falabella AF, Eaglstein WH. Tissue-engineered skin. Current status in wound healing. Am J Clin Dermatol. 2001;2:305-13.
2. Cui X, Boland T, D'Lima DD, Lotz MK. Thermal inkjet printing in tissue engineering and regenerative medicine. Recent Pat Drug Deliv Formul. 2012;6:149-55.
3.Yanez, M., Rincon, J., De Maria, C., Cortez, P., Günther, M., & Boland, T. Printed Cellular Scaffold Using Self-Crosslinking Agents. Journal of Imaging Science and Technology. 2012; 040506-1-040506-5.

Acknowledgements

The Metallurgical Engineering Department at UTEP, funding by a grant Loya to UTEP, and Texas Higher Education Coordinating Board are acknowledged. We would like to thank the staff of the Cell Culture and High Throughput Screening (HTS) Core Facility, Border Biomedical Research Center of the University of Texas at El Paso for services and facilities provided, especially to Dr. Armando Varela for his support during the immunohistochemical testing.

Probing cell-biomaterial and tissue-tissue interactions via 3D assembly of engineered cartilage micro-tissues

Woodfield TBF[1,2], Schon BS[1,2], Aigner E[3], and Hooper GJ[1]

[1] Christchurch Regenerative Medicine and Tissue Engineering (CReaTE) Group, Department of Orthopaedic Surgery and Musculoskeletal Medicine, University of Otago Christchurch, New Zealand
[2] Centre for Bioengineering & Nanomedicine, University of Otago Christchurch, New Zealand
[3] University of Applied Sciences Technikum Vienna, Austria

Introduction

Engineering of complex three-dimensional (3D) tissues requires meeting a challenging set of interdependent scaffold design and cellular criteria, making optimization of individual components difficult. Aggregate or micro-tissue based technologies are becoming increasingly popular as a method for engineering various tissues and organs [1, 2]. In this approach, cells at high density are stimulated to form micro-tissues, which can subsequently be used to print or assemble 3D tissue constructs.

We describe a 3D micro-tissue-based biofabrication model based around human chondrocyte pellet cultures to investigate cell differentiation, tissue growth and cell-biomaterial interaction behaviour in microtissues assembled in 3D-printed scaffolds, aimed at articular cartilage repair [3]. Here, the tissue is reduced to several modular components which can be separately optimized, offering opportunities to uncouple scaffold and cellular/extracellular matrix components to investigate cell differentiation, tissue growth and cell-biomaterial interaction behaviour, aimed at articular cartilage repair.

The goal of this study was to investigate interactions between 3D micro-tissues or the surrounding scaffold; and how these interactions influence engineered construct design, time course, and integration with native tissue.

Materials and Methods

Microtissues were fabricated using high-throughput methods from human mesenchymal stromal cells, articular chondrocytes or co-cultures of the two, and placed within a 3D-plotted scaffold.

Human articular chondrocytes were isolated from native tissue, expanded, and re-differentiated in pellet cultures (0.25×10^6 cells/pellet) for 7 days to form Ø 1 mm microtissues. These were assembled into precisely designed model 3D polyethylene glycol terephthalate – polybutylene terephthalate scaffolds (PEGT-PBT; PEG MW:300, wt%PEGT: 55, wt%PBT: 45), and cultured in fetal bovine serum-containing (adherent) and serum-free (non-adherent) conditions. Scaffolds either contained one micro-tissue in an individual pore to probe microtissue-biomaterial interactions, or with two microtissues adjacently constrained to examine inter-microtissue fusion kinetics and influences in the presence or absence of exogenous factors (e.g. TGFβ1, FGF, ascorbic acid-2-phosphate (AsAP), insulin-transferrin-selenium (ITS)).

Results and Discussion

Cell-biomaterial interactions – cell adhesion assays and SEM indicated cell adhesion was significantly reduced in non-adhesive conditions. Interestingly, 3D micro-tissue assembly in adhesive scaffolds showed no significant differences in re-differentiation capacity and tissue quality as detected by GAG content, cell number, or expression of type-I and type-II collagen compared to non-adhesive scaffolds.

Fusion: kinetics, influences, and contributing mechanisms – tissue fusion progressed rapidly (from 1 day). Micro-tissue contact was required for fusion to occur, and the increase in micro-tissue diameter over time was associated with matrix content. Where conditions altered matrix production (-AsAP, -TGFβ1) or proliferation (+FGF) individually, fusion of tissues was unaffected; however if both were affected (-ITS), this reduced fusion between microtissues.

These results, in combination with the fibrous appearance of tissue formed in the tissue interfaces, indicated overall growth in size of the tissues and cell proliferation at the interface were responsible for fusion.

Conclusions

3D micro-tissue assembly for articular tissue engineering can produce good quality tissue when in contact with either an adhesive or non-adhesive scaffold surface. Individual microtissues can fuse rapidly; fusion is influenced by exogenous factors and is due to matrix production in combination with proliferation at the tissue interface. This experiment demonstrates in vitro culture time and soluble factors are important for an assembled construct based on cartilage microtissues, while scaffold material is less important. It also gives clues for enhancing implant integration and design.

References

1. Dean, D.M., Napolitano, A.P., Youssef, J., Morgan, J.R. (2007). Rods, tori, and honeycombs: the directed self-assembly of microtissues with prescribed microscale geometries. *FASEB Journal* 21, 4005-4012.

2. McGuigan, A.P., Sefton, M.V. (2007). Design and fabrication of sub-mm-sized modules containing encapsulated cells for modular tissue engineering. *Tissue Eng* 13, 1069-1078.

3. Schon, B., Schrobback, K., van der Ven, M., Stroebel, S., Hooper, G., Woodfield, T. (2012). Validation of a high-throughput microtissue fabrication process for 3D assembly of tissue engineered cartilage constructs. *Cell Tissue Res* 347, 629-642.

Acknowledgements

We acknowledge funding from the AO Foundation (Davos, Switzerland S-08-81W) and the Royal Society of New Zealand Rutherford Discovery Fellowship (TW).

Microfabrication of Novel Modular Design Having Hollow Structures as Building Units and Their Feasibility in Liver Tissue Engineering

S. Sutoko[a], Y. Pang[a], Y. Horimoto[b], T. Niino[a], Y. Sakai[a]
[a] Institute of Industrial Science, University of Tokyo, Komaba 4-6-1, Meguro-ku, Tokyo, 153-8505, Japan
[b] Graduate School of Engineering, Shibaura Institute of Technology, Shibaura 3-9-14, Minato-ku, Tokyo, 108-8548, Japan

Introduction

To develop the clinically minimum required volume equivalent as 20-30% or 500 cm^3 of average liver volume for preserving the homeostasis[1], the modular assembly concept is promising over the top-down approach hindered by the spatial organization[2]. Provided by the randomized packed modules as smallest building blocks, the formed interstitial gaps establish the channel-like-structure and become the distinguished point for maintaining the sustainability of medium transport directing to higher cell viability and functions. The existed attempt utilizing collagen gel as module material was easily be deformed and collapse[3,4] due to susceptible mechanical stress leading to module adhesion to each others and further vanished interstitial gap.

The replacement of collagen gel and advanced designated structure are being the main ideas. The usage of rigid polymer such as biodegradable poly-glycolic acid (PGA) can support the easier fabrication of designated structure. We expect the familiar used PGA material having the beneficial in fabrication step and further the novel structure provided by the hollow structure in PGA tube modules will perform the enhanced fluidity because of increasing prepared flow channel. The novel and advantageous modular unit implementation is able to encourage the feasibility of liver tissue engineering showed in high cell viability and favorable quantified hepatic function such as albumin production.

Materials and Methods

The fabricated PGA modules through selective laser sintering (SLS) method as shown in Fig.1 is employed by around 50% porosity. Each module was prepared and proceeded for cell culture in sequence of module sterilization, collagen coating, overnight inoculation in 90 rpm rotary shaker, decreasing the rotational speed into 45 rpm and maintaining culture for 14 days by daily culture replenishment. The number of attached cells on module were measured based on the spectrophotometry of DAPI-stained DNA of homogenized cells and standardized DNA amount to cell number correlation. The cell viability on the final day of culture was analyzed via PI and calcein staining under confocal microscope and subsequently quantified using ImageJ software by comparing the detected live cells presented in green area and otherwise the dead cells shown in red area. Additionally, the daily albumin production as one of hepatic functions was examined using ELISA method and measured in 450 nm.

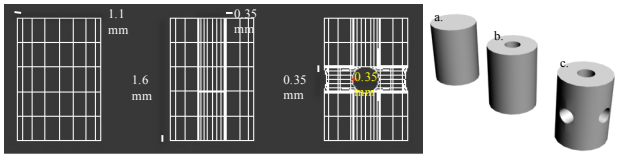

Figure 1 The novel fabricated design of modules 1) cylindrical module, b) hollow canal module, and c) intersecting pores module

Results and Discussion

Overlaid collagen on the PGA module empowered the attachment of hepatic cell line, Hep G2. Provided by the high porosity around 50% and hollow structure(s) encouraging the cell suspension distribution, the intersecting pores module supported the desired cell attachment as 5.3×10^7 cells/cm^3 whereas cylindrical and hollow canal handed over the result $3.2 - 3.6 \times 10^7$ cells/cm^3. The reinforced intersecting pores module can be commensurate around 20% of *in-vivo* cell density (2.5×10^8 cells/cm^3). After 14 days cell culture, the viability of remained cells on all type of assessed modules presented promising outcomes in range 77% - 85% confirming the sustainable medium and oxygen transfer. These results are also emphasized by the daily progressive albumin production for each type of modules, yet the intersecting pores module surpasses 28% and 30% of albumin production for cylindrical and hollow canal modules respectively. The results promote our previous hypothesis of beneficial rigid designated novel PGA module by lingered channel structures attained from hollow structures led to improved distribution.

Conclusion

The accomplished experiments confirm our initial hypothesis regarding to the opportunity of utilization PGA as module material associated by novel design models in liver tissue engineering. PGA contributes its rigidity for supporting the design and high porosity, it, thus, enhances the cell loading and medium fluidity inducing increased viability. The betterment and further research can be done by conducting the perfusion culture in a bed construction or even adjoined with endothelial cell lines for exploring the expected vascularization.

References

[1] Naruse, K.; Nagashima, H.; Sakai, Y.; Kokudo, N.; Makuuchi, M. *Surg. Today* 2005; **35**: 507-517.
[2] Liu, J.S.; Gartner, Z.J. *Trends in Cell Biology* 2012; **22** (12): 683-691.
[3] McGuigan, A.P.; Sefton, M.V. *Proceeding of the National Academy of Science* 2006; **103** (31): 11461-11466.
[4] Khan, O.F.; Sefton, M.V. *Biomaterials* 2010; **31**: 8254-8261.

Posters

3D printing of biocompatible acellular auricular implant using dual scaled hydrid technology combining fused deposition modeling with electrospinning.

Rodrigo Rezende, Marcos Antonio Sabado, Vladimir Kasyanov, Leandra Baptista, Karina da Silva, Pedro Noritomi, Frederico Sena, Xuejun Wen, Jorge V.L. da Silva, Vladimir Mironov
CTI, Campinas, SP, Brazil; InMetro, Xerem, RJ, Brazil;
Riga Stradins University and Riga Technical University, Riga, Latvia;
University of Caracas, Venezuela; Virginia Commonwealth University, Virginia, USA

Introduction

There is a growing consensus that a cell-based therapy and tissue engineering products are very costly and a subject of long and difficult regulatory approval. Recently, the cost-effective approach based on using acellular biomaterials have been suggested as a cost-effective alternative to cells-based therapy[1]. It have been suggested that acellular biomaterials could be easier to approve for clinical use and, especially, functional or drug-eluting acellular biomaterials inducing endogenous regeneration using cell homing could be potentially an optimal cost-effective approach in regenerative medicine with moderate (although not ideal) positive clinical outcome [1].

The dual-scaled hydrid scaffold fabrication technology based on combination of 3D printing (fused deposition modeling) and electrospining have been recently introduced. We report here the design, fabrication, mechanical testing, in vitro and in vivo biocompatibility testing of novel auricular implants for treatment microtia fabricated by dual scaled hydrid scaffold fabrication technology.

Materials and Methods

The dual scaled hybrid fabrication technology have been used for fabrication auricular implant using custom designed 3D printer and electrospinning apparatus from polyurethane. Computer-aided design (CAD) of external human ear shape of volunteers have been generated using commercial laser scanner and transformed in STL file using open source software (inVesalius, CTI, Brazil). Computer simulation using finite element analysis (FEA) have been used to find optimal mechanically biomimetic geometrical design for auricular implant. Mechanical testing of human cadaveric auricular cartilage and fabricated implant have been performed using three points flexure test. The *in vitro* biocompatibillity have been estimated using tissue spheroids attachment and spreading test. The *in vivo* implant biocompatibility and shape retention was tested by subcutaneous implantation in rats.

Results and Discussion

Auricular implants have been designed and fabricated using dual-scaled fabrication technology combining 3D printing and electrospinning of synthetic polyurethane (Fig1). It have been shown that fabricated auricular implants have biomimetic material properties comparable with material properties of human cadaveric auricular cartilage (Fig.2). Fabricated auricular dual-scaled implants demonstrated good *in vitro* biocompatibility. Electrospun matrices enhance tissue spheroids attachment and spreading. The good biocompatibility and shape retention have been shown *in vivo* after implantation (Fig.3)

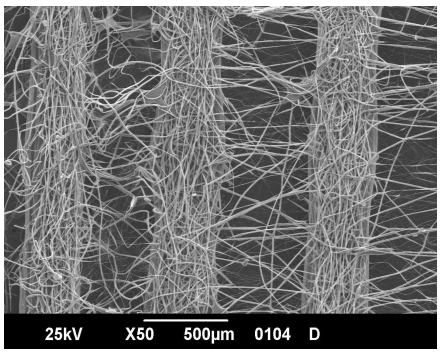

Figure 1. SEM of dual scaled scaffold fabricated by fused deposition modeling and electrospinning

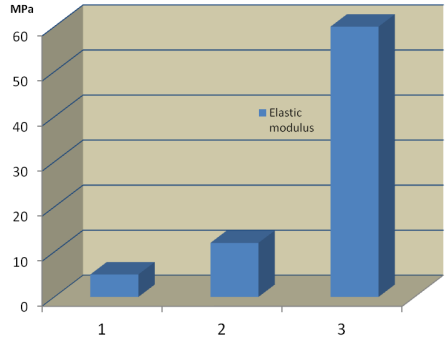

Figure 2. Material properties of human auricular cartilage(1), polyurethane printed implant (2), and porous polyethylene (Porex) (3)

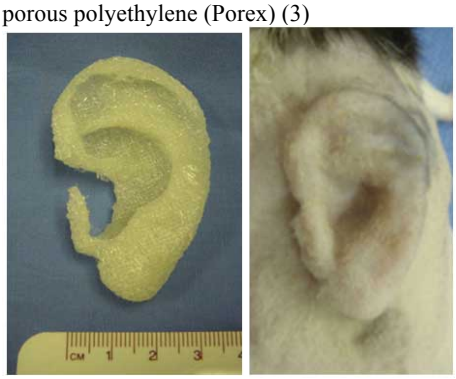

Figure 3. Fabricated auricular implant before (left) and after implatation (right)

Conclusions

Biomimetic compliant acellular auricular dual scaled hydrid implant have been designed, fabricated and tested in vitro and in vivo.

References

1. Burdick JA et al. Sci Transl Med. 2013 13;5(176):176

Acknowledgements

This study was partly funded by Brazilian funding agencies CNPq and FAPESP

A nature-inspired cell culture platform for studying cell-patterned PDMS surface interaction

Hyeon Jun Hong, Sung Jea Park, Moon-Hee Na and Dong Sung Kim
Department of Mechanical Engineering, Pohang University of Science and Technology (POSTECH), South Korea

Introduction

Recently, many biological researches have focused on surface topographical effect on cell behaviors like proliferation, differentiation or alignment. Though PDMS (Polydimethylsiloxane) patterns with microstructures are widely used in the cell topological study due to its biocompatibility and simple fabrication process [1] the cell culturing procedures using PDMS patterns are time-consuming and laborious because a well–plate to be containing PDMS patterns should be replaced in every media-exchanges from a cell seeding step. Therefore, it should be helpful to develop a cell culture platform based on PDMS patterns that enable us to facilitate the exchange of media and well-plate.

Our approach for achieving a new concept of a cell culture platform is to mimic the floating flower. In previous study [2], it is reported that the flower shaped thin sheet can be used to grab and deposit a liquid using the elasto-capillarity. In this study, we proposed a simple method to fabricate flower shaped PDMS sheets with micro-patterns as the culture platform for studying cell-surface topography interaction.

Materials and Methods

The patterned PDMS sheet fabricated through a PDMS replica molding process. A mold system was composed of the top and bottom molds as shown in Fig. 1(a). The top mold was manufactured with the help of micro-machining using PMMA plate to have a flower shaped cavity. The dimension of flower shape was designed by referring the previous study [2]. Total length of 40 mm and the thickness of 0.4 mm were optimized with considering the surface tension of cell culture media and elasticity of PDMS. The center hole that will generate the holder was also machined in top mold. In the bottom mold fabrication, micro-patterns with square pillars having width of 50 μm and height of 10 μm were generated by UV-photolithography on PMMA plate. The fitting core and cavity for sealing of the mold system were also machined on the top and bottom molds, respectively.

For the PDMS replication, PDMS pre-polymer mixed with a curing agent was injected through the center hole of the assembled mold system which was clamped for sealing and then cured in 65˚C for 4 h (Fig. 1(a)). After the curing, the flower shaped PDMS sheets with the patterns were peeled off from the PMMA mold (Fig. 1(b)).

Results and Discussion

The micro-patterns were successfully fabricated on the surface of PDMS sheet, as shown in the scanning electron microscopy (SEM) image in Fig. 1(c).

Using the replicated flower shaped PDMS sheets, the experiments of grabbing media were carried out. As shown in Fig. 2(a), the PDMS sheet captured the media stably and repeatedly.

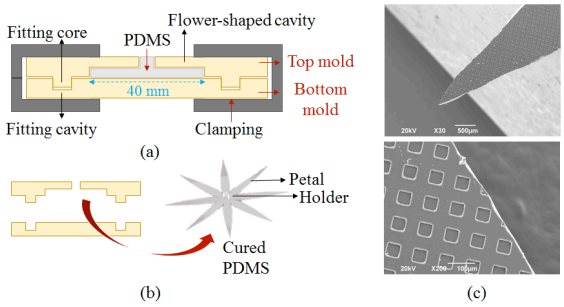

Figure 1. (a)-(b) the PDMS replica molding process, (c) SEM images of micro-patters on the PDMS sheet.

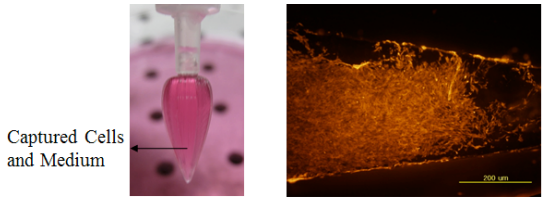

Figure 2. (a) The cells and media captured with the PDMS sheet, (b) Cultured MG-63 cells.

As a proof of concept, MG-63 osteosarcoma cells were cultured on the flower shaped PDMS sheet with flat surface for 3 days. Fig. 2(b) shows the cultured MG-63 cells were well attached on the PDMS sheet.

The results revealed that the flower shaped PDMS sheet with micro-patterns could be fabricated via the simple replica-molding process. Furthermore, as compared to the conventional PDMS patterns, the flower shaped PDMS sheet could simplify the cell procedure with no additional process such as well-plate exchange.

Conclusions

In this study, we suggested a simple fabrication method for a new concept of cell culture platform. Inspired by the nature, the micro-patterned PDMS sheets were fabricated in form of a flower shape through the simple replication process. Using the PDMS sheet, cell culture procedures could be simplified.

References

[1] Kim EJ, Boehm CA, Mata A, Fleischman AJ, Muschler GF, Roy S. 2010 Post microtextures accelerate cell proliferation and osteogenesis *Acta Biomater*. 6 160-9
[2] Reis PM, Hure J, Jung S, Bush JWM, Clanet C 2010 Grabbing water *Soft Matter* 6 5705-8

Acknowledgements

This work was supported by the Industrial Core Technology Development Program funded by the Ministry of Knowledge Economy (No.10041913).

Customized biomimetic scaffolds created by indirect three-dimensional printing for tissue engineering

Ju-Yeon Lee[a], Bogyu Choi[a], Benjamin Wu[a,b], Min Lee[a,b]
[a]Division of Advanced Prosthodontics, [b]Department of Bioengineering
University of California, Los Angeles, California 90095

Introduction

Three-dimensional printing (3DP) is a rapid prototyping technique that can create complex 3D structures by inkjet printing of a liquid binder onto powder biomaterials for tissue engineering scaffolds [1-2]. Direct fabrication of scaffolds from 3DP, however, imposes a limitation on material choices by manufacturing processes. In this study, we report an indirect 3DP approach wherein a positive replica of desired shapes was printed using gelatin particles, and the final scaffold was directly produced from the printed mold.

Materials and Methods

The anatomic shape of mandibular condyle was isolated from the CT scan using software (Mimics). CAD software (Solidworks) was used to create 2 mm orthogonal intersecting channels. The objects were built sequentially on a 3DP machine (Z402) using gelatin powders.

PCL scaffolds were fabricated by infiltrating the printed gelatin molds with polycaprolactone (PCL) in chloroform (7% w/w). Molds were removed by placing them in deionized water at 50 °C. For Chitosan (CH) fabrication, the obtained PCL scaffolds were infiltrated with CH solution, crosslinked with chondroitin sulfate and pentasodium tripolyphosphate solution. The scaffolds were neutralized, sterilized and lyophilized overnight. Scaffolds were etched to make the surface hydrophilic and incubated in SBF 1 and 2 for apatite coating.

The morphology of scaffolds was observed by scanning electron microscopy (SEM). The chemical structure of the scaffolds was analyzed using ATR-FTIR before and after apatite coating.

Mouse bone marrow stromal cells (BMSCs) were used to check biocompatibility of scaffolds. To observe the proliferation of BMSC, samples were stained using calcein solution and observed using a fluorescence microscope. The AlamarBlue assay kit was used to further measure the proliferation of cells on the scaffolds.

Results and Discussion

To create patient-specific scaffolds that match precisely to a patient's external contours, we integrated our indirect 3DP technique with imaging technologies (figure 1a). To test the ability of the technique to precisely control the internal morphology of the scaffolds, we created orthogonal interconnected channels within the scaffolds using computer-aided-design models (figure 1b). In this study, we have successfully developed casting molds using gelatin particles, which are more biocompatible compared to previous plaster molds and can be easily removed in water after casting (figure 1c). The printed gelatin molds were successfully cast with synthetic and natural biomaterials widely used for bone regeneration such as PCL and CH (figure 1d-e). Because very few biomaterials are truly osteoinductive, we modified inert 3D printed materials with bioactive apatite coating. The feasibility of these scaffolds to support cell growth was investigated using BMSCs. BMSCs showed good viability of >95% in all scaffolds over the 14 days culture period. Apatite-coated scaffolds enhanced spreading and proliferation of BMSC seeded on the scaffolds compared to non-coated scaffolds as assessed by live/dead and alamarBlue assays.

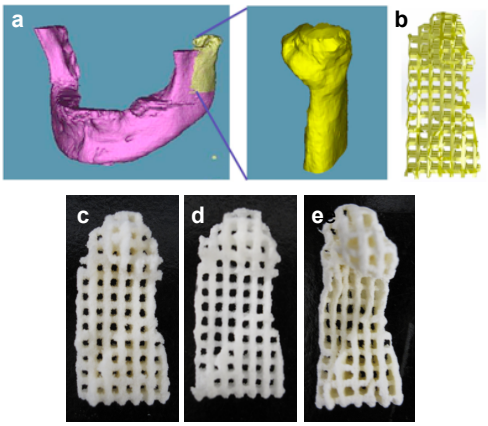

Figure 1. Fabrication of custom scaffolds by indirect 3D printing technique. (a) 3D reconstruction of human Condyle from CT images, (b) creating of microchannels using CAD modeling, (c) 3D printed gelatin preform, (d) 3D printed PCL scaffold, (e) 3D printed chitosan scaffold.

Conclusions

In this study, we demonstrated an indirect 3DP process for the fabrication of custom scaffolds with a specific anatomic shape and optimized internal architecture by the infiltration of common biodegradable polymer solutions into gelatin porogens and a subsequent leaching technique. The created scaffolds were cytocompatible and their bioactivity was further improved by post-surface treatment. Further investigations are needed to determine if the present scaffolds can induce differentiation of cells *in vitro* and support functional tissue regeneration *in vivo*. This technique provides a promising new strategy to engineer multifunctional scaffolds for the regeneration of complex damaged tissues.

References

[1] Lee M, Dunn J C Y and Wu B M 2005 *Biomaterials* **26** 4281-9
[2] Lee M, Wu B M and Dunn J C Y 2008 *Journal of Biomedical Materials Research Part A* **87A** 1010-6

Acknowledgements

This work was supported by the National Institutes of Health grants R01 AR060213 and R21 DE021819, the International Association for Dental Research, and the Academy of Osseointegration.

Mesenchymal Stem Cells guide Endothelial Cells in a model organized by Laser-Assisted Bioprinting.

Manuela Medina[1], Emeline Pagès[1], Murielle Rémy[1], Reine Bareille[1], Joëlle Amédée- Vilamitjana[1], Fabien Guillemot[1], Raphaël Devillard[1]

[1] *INSERM U1026 - Tissue Bioengineering, University Bordeaux Segalen, 33076 Bordeaux, France*

Introduction

The construction of complex tissues including a vascular network is a challenging issue in tissue engineering. The lack of vascularization during the *in vitro* growth and development of bones remains one of the main problems that must be overcome (1). *In vitro* prevascularization by the use of endothelial cells (ECs) and mesenchymal stem cells (MSCs) in coculture is acquiring much more importance. However, tissues are a combination of small repeating units assembled together. To allow in vitro building of tissue-like structures there is a necessity to create and manipulate the microenvironment consisting of biomolecular gradients and cell-cell interactions. The aim of this study is to use the laser-assisted bioprinting technique to investigate the optimal pattern and distance at which human umbilical endothelial cells (HUVECs) and human bone marrow stem cells (HBMSCs), alone or in coculture, will form an aligned structure and hence a functional micro-vascular structure.

Materials and Methods

The laser-assisted bioprinting technique was used to develop all the experiments. Both types of cells were printed in monoculture and coculture in a hydrogel of collagen type 1. Cell viability was verified by live/dead assay and the F actin staining showed the cell spreading. Two specific markers of ECs, vWF and CD31, were used to show that the printing and patterning procedures did not affected cell phenotype.

Results and Discussion

Both HUVECs and HBMSCs showed a beginning of an alignment at 6 and 24 hours, respectively; while in coculture they showed a complete alignment at 24 hours where HBMSCs conduce HUVECs to stay over them (Fig 1).

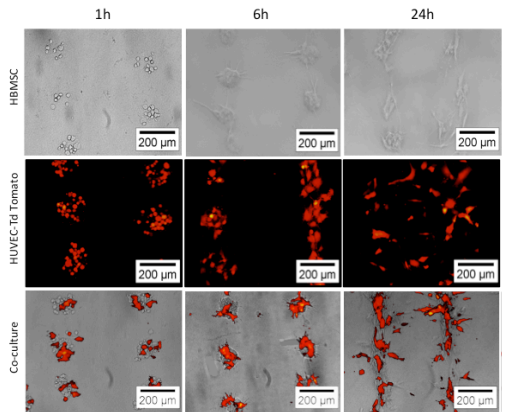

Figure 1. Follow-up over time of HBMSCs (upper line), HUVECs-TdTomato (middle line) and HBMSCs – HUVEC Tomato (lower line) from 1 to 48 hours post-printing, using an inverted microscope (Axiovert). In red: HUVECs, expressing Td-Tomato. Images were representative of n=7 experiments. Distance between segments: 500 µm.

Specific markers of ECs, such as von Willebrand Factor (vWF) and CD31 were expressed post-printing in monocultured and cocultured HUVECs. HBMSCs guide HUVECs organization in a coculture model (Fig 2).

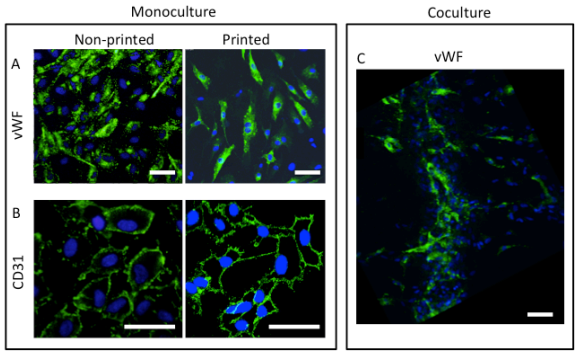

Figure 2. Immunofluorescence images of printed and non-printed HUVECs, demonstrating that they preserved their specific endothelial markers. Von Willebrand expression (vWF, green) of non-printed and printed cells after 48 hours **(A)**. CD31 expression (green) of non-printed cells after 48 hours and of printed cells after 6 hours **(B).** In coculture, HUVECs were stained with the vWF 48 hours post-printing, and the nuclei were labeled in both HUVECs and HBMSCs **(C)**. The nuclei (in blue) were also labeled in images **(A-C)**. Images were representative of n=3 experiments. Scale bar: 50 µm

Conclusions

MSCs alignment plays a role in ECs organization when both are printed in coculture. The bioprinting is a promising tool to study cell behavior with great accuracy as well for developing innovative strategies for tissue fabrication.

References

1. Grellier M, Bordenave L, Amédée J. Cell-to-cell communication between osteogenic and endothelial lineages: implications for tissue engineering. Trends in Biotechnology. 2009 august 14; 27 (10): p. 562-571.

Acknowledgements

To the INSERM for financial support.

Nanostructured Pluronic hydrogels for bioprinting

Mischa Müller, Marcy Zenobi-Wong

Introduction

An ideal bio-ink for extrusion printing should be liquid at the beginning to mix it freely with other polymers, peptides or cells. After mixing, the flow behavior must be compatible with an extrusion printing process. For printing fidelity, immediate cessation of flow upon deposition is necessary. In case of cartilage bioprinting, the ink should also be cytocompatible and induce chondrogenesis.

The thermoresponsive block co-polymer poly(ethylene oxide)-poly(propylene oxide)-poly(ethylene oxide) (Pluronic) is fulfilling the requirements for a good bioink regarding its rheological properties, but has been deterred from widespread use due to its cytotoxic effects at printable concentrations[1]. At lower concentrations however, the cytotoxic effects are not present[2].

We investigated blends of acrylated and unmodified Pluronics for bioprinting applications. For the printing process, the initial Pluronic concentration is suitable for extrusion bioprinting. After crosslinking of the printed construct, unmodified Pluronic is eluted out and the final Pluronic concentration is in the range where no cytotoxic effects are present. We hypothesize that this method creates a nanostructured hydrogels that improve cell survival compared to higher concentrated Pluronic gels.

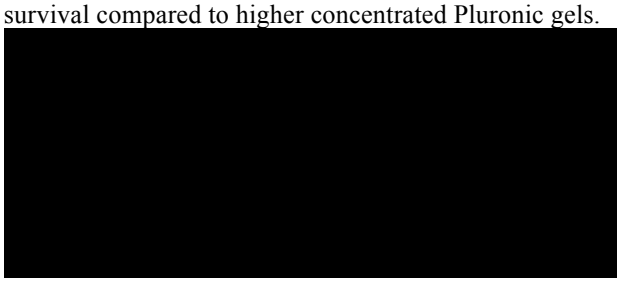

Figure 1. Schematic drawing of nanostructured Pluronic hydrogels. The bio-ink can also be mixed with photocrosslinkable biopolymers such as chondroitin sulfate or hyaluronan

Materials and Methods

Acrylated Pluronic F108 (PF108-DA) was synthesized as described elsewhere[3]. The blends of acrylated and unmodified Pluronics were analyzed with an Anton Paar MCR301 rheometer utilizing a cone-plate (to measure flow behavior) or plate-plate geometry (for mechanical testing). Flow curves were recorded to test the printability of the blends. Temperature ramps and UV crosslinking under oscillation were performed to investigate the gelation temperatures and UV-crosslinking kinetics. Chondrocytes were analyzed with an optical microscope at 1 and 7 days after the photoencapsulation in the PF108 hydrogel blends. 1.2% Alginate beads were used as a control. A bioprinter (BioFactory,RegenHu, Villaz-St-Pierre, Switzerland) equipped with a solenoid valve and a needle with 300 µm diameter was used create the hydrogel scaffolds.

Results and Discussion

Cells encapsulated in pure Pluronic F108-DA hydrogels show decreasing cell viability with increasing concentration (5,10 and 15%). When part of the Pluronics-DA is replaced with unmodified Pluronics, the cell viability can be improved while maintaining the printability and ability to from a macroscopically cross-linked gel. The blends also seem to be less cytotoxic than lower concentrated pure F108-DA gels. While the cells in the 5 % Pluronic F108-DA have a smooth morphology similar to cells in alginate beads at day 1, the morphology changed over the course of a week to a more rough one. In gels where 10% unmodified Pluronic F108 was added, the change in morphology was less pronounced (see Figure 2).

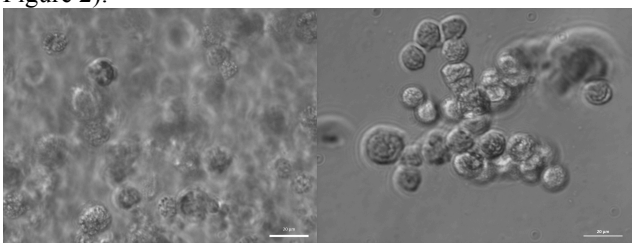

Figure 2. Microscopy images of bovine chondrocytes embedded in Pluronic hydrogels 8 days after encapsulation. While in the pure 5% Pluronic F108-DA samples the cells show a rough morphology, cells in 5% Pluronic F108-DA gels that had 10% unmodified F108 added appear more smooth.

We assume that there are two possible reasons for the improved viability after 8 days. Elution of the unmodified Pluronics might lead to the creation of a porous network that is non-existant in the pure 5% F108-DA sample. Another possibility is that there is competitive adsorption between the more cytotoxcic F108-DA (shown in 2D experiments) and the unmodified F108 on the cell surface.

Conclusions

Replacement of diacrylated F108 with its unmodified version improves the cell viability while maintaining the printability of the bioink. Addition of photocrosslinkable biopolymers could improve viability further and include degradable structures into the hydrogel network

References

1. Fedorovich et al. *Biomacromolecules* 2009, 10, 1689–1696
2. Khattak et al. *Tissue Engineering* 2005, 11, 974-983
3. A. Sosnik, et al. *J. Biomater. Sci. Polymer. Edn* 2003, 14, 227-239

Acknowledgements

The work was funded European Union Seventh Framework Programme (FP7/2007-2013) under grant agreement n^{0}NMP4-SL-2009-229292.

Synthesis of Alginate-Polypyrrole Ionomeric Composites

Timothy Hanks[1,2], Campbell Yore[1], Cassandra Wright[1], Trent Pannell[1], BinBin Zhang[2],
[1]Department of Chemistry, Furman University, USA
[2]Intelligent Polymer Research Institute, University of Wollongong, Australia

Introduction

Alginic acid and its salts (alginates) are linear carbohydrate co-polymers that are typically extracted from seaweed. The material is a block copolymer of β-D-mannuronate (M) and α-L-guluronate (G), with the latter residue playing an important role in the presence of certain metal ions having a charge of two or greater. Ca^{2+}, for example, acts as an efficient cross-linker that results in a gel with variable viscoelasticity. The rigidity of the material is largely a function of the ion density and distribution in the host polymer. We are interested in composites of alginates with polycationic intrinsically conducting polymers (ICPs), particularly polypyrrole PPy) and poly(3,4-ethylenedioxythiophene) (PEDOT) as scaffolds for neural tissue growth and regeneration.

Materials and Methods

All reagents were purchase from Sigma-Aldrich and used as received except as indicated. Pyrrole was purified by distillation over molecular sieves under nitrogen and stored a 0 °C. Insert buffer information. IR data were collected on cast films using an ATR attachment. Rheometry data were collected with a quartz crystal microbalance and a flow viscometer at room temperature. Conductivity was measured using the four point probe method.

Composites were prepared by dissolving sodium alginate in 50 mL of DI water or an aqueous buffer to a concentration of 2% w/v. Pyrrole (X ml) and $K_2S_2O_8$ (Y mg) were added and the solutions stirred for 48. After purification by dialysis, films were formed by evaporation of excess water under vacuum.

Results and Discussion

Polypyrrole is formed by the oxidative polymerization of pyrrole, giving an electronically conducting polycation. The reaction is typically run using $FeCl_3$ alone or in combination with a second oxidant such as a persulfate salt. It is desirable to omit the iron oxidant, but this comes at the cost of a longer reaction time. We observed that the during the course of the reaction, the viscosity of the alginate solution decreased dramatically. The alginate solutions also showed greatly decreased ability cross-link with Ca^{2+}. The polypyrrole caused much of the alginate to phase separate as a fragile gel and attempts to cast thin films from the mixture resulted in powders or delicate aggregates. The IR spectrum of the material showed the growth of a carbonyl peak at *ca.* 1725 cm^{-1} is consistent with the oxidative degradation of alginate. Control studies of alginate persulfate mixtures showed no viscocity changes or carbonyl formation.

The pyrrole polymerization generates protons and thereby lowers the pH of the reaction media during the course of the reaction. It has been shown that metal ions, elevated temperature and acidity all encourage the decomposition of persulfates into other radical oxidants. Decreasing the reaction temperature and the addition of EDTA to remove trace metal impurities in the alginate had little impact on the rheology of the material. However, increasing the pH by the addition of base or running the reaction in buffer solutions both reduced the formation of the carbonyl peak and stopped the loss of solution viscosity. These composite suspensions gelled on addition calcium chloride and upon drying, formed robust, flexible films with good electrical conductivity.

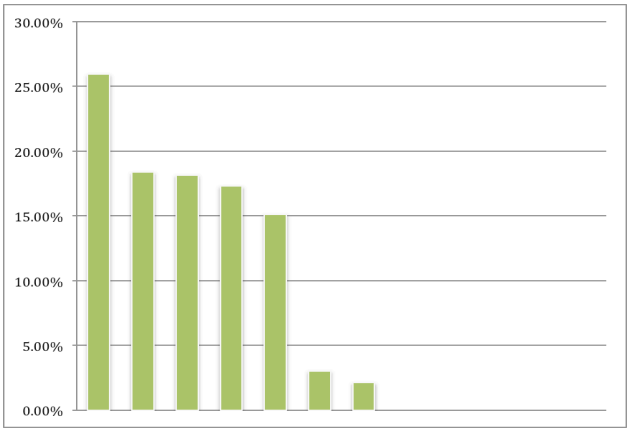

Figure 1. ATR-IR spectra of reaction products run under different conditions.

Conclusions

The control of pH during the chemical polymerization of pyrrole is key to preparing electrically conducting hydrogels with the mechanical properties necessary allow for their extrusion into 3D scaffolds for tissue engineering. Higher pH also improves the electrical conductivity of the material, probably by discouraging over oxidation. Low pH also results in cell death when the composite is used as a cellular scaffold.

References

List references cited in text. Duis aute irure dolor in reprehenderit in voluptate velit esse cillum dolore eu fugiat nulla pariatur. Excepteur sint occaecat cupidatat non proident, sunt in culpa qui officia deserunt mollit anim id est laborum magna aliqua.

Acknowledgements

This work was supported through a GEAR:RE award from South Carolina EPSCoR/IDeA. TH thanks the Australian-American Fulbright Foundation for a fellowship. CW was supported by SC-INBRE PACD fellowship; grant number P20GM103499 from the National Institute of General Medical Sciences. BZ received travel support from …

Plasma treatment of electrospun PCL nanofibers for biological property improvement

D Yan[1, 2], J Jones [2], XY Yuan [1], XH Xu [1], J Sheng [1], GQ Ma[1] and QS Yu[2]

[1] College of Materials Science and Engineering, and Tianjin Key Laboratory of Composite and Functional Materials, Tianjin University, Tianjin, 300072, China

[2] Center for Surface Science and Plasma Technology, Department of Mechanical and Aerospace Engineering, University of Missouri, Columbia, MO 65211, U.S.A.

Introduction

Due to their biodegradation, biocompatibility, and adequate mechanical properties, electrospun poly(ε-caprolactone) (PCL) nanofibers have been proposed as templates for tissue engineering scaffolds. The use of PCL for tissue engineering is limited by its hydrophobic properties, leading to a low cell loading in the initial stage of cell culture and resulting in low cell attachment and proliferation. Therefore, it is essential to improve PCL surface wettability in order to overcome the problems mentioned above. Plasma treatment using low-temperature plasmas is a simple and effective method for the surface modification of a variety of materials without affecting the material bulk properties [1].

Materials and Methods

The electrospinning setup used in our experiments is a typical device including a high-voltage power supply (ES50P-5W, Gamma High Voltage Research, Ormond Beach, FL, USA), a spinneret, and a collector. Poly (ε-caprolactone) (PCL, Aldrich, MW = 80,000) was dissolved in a mixture of chloroform and methanol (3:1 by volume) to prepare a 9 wt% PCL solution for electrospinning. The voltage used for electrospinning was 20kV, and the collection distance was 9 cm. PCL nanofibers were exposed to gas plasmas created in a bell-jar plasma reactor under low pressure using a radio frequency (RF) power supply at 13.56 MHz for plasma treatment to modify their surfaces. The gas flow rates used in this study were 1 sccm + 1 sccm for Ar + O2 mixture, 2 sccm + 1 sccm for NH3 + O2 mixture, and 1 sccm + 3 sccm for N2 + H2 mixture. The 1:3 ratio for N2+H2 mixture was adopted because the N:H=1:3 ratio is the same as NH3 gas, which is corrosive and problematic for plasma process. The PCL nanofiber sufaces were characterized using surface contact angle measurements, scanning electron microscopy (SEM), X-ray photoelectron spectroscopy (XPS), tensile tests, and cell culture using mouse osteoblast cells (MC3T3-E1).

Results and Discussion

It was found that plasma treatment resulted in a significant increase in surface hydrophilicity of the PCL nanofibers, with the water contact angle reduced from ~135° to 0°. XPS surface characterization indicates that the plasma treatment introduced new functional and polar groups on the fiber surface. Tensile test results show that, after the plasma treatment, the ultimate tensile strength and the ultimate strain of both the PCL nanofiber random mats and aligned meshes were reduced compared to those of the untreated controls, which indicates that the plasma etching effect occurred on the PCL nanofiber surfaces. As shown in Figure 1, when cultured with mouse osteoblast cells (MC3T3-E1), the plasma-treated PCL nanofiber random mats and aligned meshes yielded much higher cell proliferation rates compared to those obtained for the untreated controls. Environmental SEM examination shows that the plasma treatment significantly enhanced cell growth along the aligned PCL nanofibers.

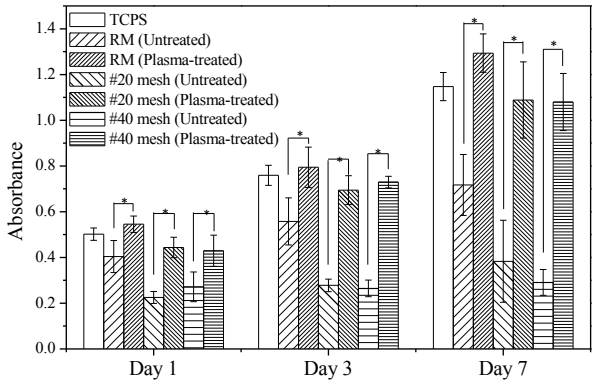

Figure 1. MTT results after 1, 3, and 7 days of cell culture using MC3T3-E1 cells on untreated and plasma-treated PCL nanofibers and the untreated controls.

Conclusions

Plasma treatment made the hydrophobic PCL RMs and meshes extremely hydrophilic, as evidenced by a water surface contact angle of 0° and rapid water penetration and spreading observed during the water contact angle measurement. Cell culture results demonstrate that, in comparison with the untreated controls, the proliferation rates of osteoblast cells were significantly enhanced on plasma treated PCL naofibers. These results indicate that plasma treatment of the electrospun nanofibers has great potential for tissue engineering applications. It should be noted that plasma treatment can induce certain structural damage on the nanofibers and care should thus be taken when is used for surface modification of PCL nanofibers.

References

[1] Martins A, Pinho E D, Faria S, Pashkuleva I, Marques A P, Reis R L and Neves N M 2009 Surface modification of electrospun polycaprolactone nanofiber meshes by plasma treatment to enhance biological performance Small 5 1195-206.

Acknowledgements

The authors would like to thank Prof. James Lee of Department of Biological Engineering at University of Missouri for his kind suggestions to the work and allowing us to perform cell culture in his research lab.

The arrow-headed lockyballs (velospheres) locking with electrospun matrices for rapid biofabrication of 3D tissue constructs.

Paulius Danilevicius[5], Frederico D.A.S. Pereira[1], Rodrigo A. Rezende[1], Leandra Baptista[2], Karina da Silva[2], Anna Mitraki[5], Maria Chatzinikolaidou[5], Vladimir Kasyanov[3], Marcos Antonio Sabino[1,4], Jorge V. L. da Silva[1], Maria Farsari[5], Vladimir Mironov[1,5]

[1]Center for Information Technology Renato Archer (CTI), Campinas, SP, Brazil; [2]InMetro, Xerem, RJ, Brazil; [3]Riga Stradins University and Riga Technical University, Riga, Latvia; [4]Simon Bolivar University, Caracas, Venezuela; [5]University of Crete and FORTH-IESL, Heraklion, Crete, Greece

Introduction

There are two distinct premises in tissue engineering: i) bottom-up modular directed tissue self-assembly and ii) solid scaffold based approach (1). There is a growing consensus that a third strategy based on the integration of advantages of a directed tissue self-assembly approach with a conventional solid scaffold-based approach could be a potential optimal solution (1,2). The concept of tissue spheroids encaged into interlockable microscaffolds which combines advantages of both main distinct approaches in tissue engineering as a variant of desirable third strategy and as a new technological platform for rapid *in situ* 3D tissue biofabrication has been recently introduced (3). We report here the design, fabrication of second generation of arrow-headed microscaffolds or velospheres (from Greek word ***βέλος*** – arrow) interlocking with electrospun matrices for rapid *in situ* biofabrication of multilayered 3D tissue constructs.

Materials and Methods

Arrow-headed microscaffolds or velospheres have been designed and fabricated using two photon polymerization of organically modified photo-sensitive biomaterials. Synthetic electrospun matrix has been fabricated using home made electrospun apparatus. The lockyballs have been cellularized with human adipose tissue derived stem cells using micromolded non-adhesive agarose hydrogel. Interlocking of arrow-headed velospheres with elecrospun matrixes has been tested. Viability of cell encaged in velospheres has been tested using standard vitality tests. Scanning electron microscopy has been used to study morphology and geometry of fabricated velospheres and their interaction with electrospun marices.

Results and Discussion

Arrow-headed microscaffolds or velospheres have been designed and fabricated using two photon polymerization (Fig.1). It has been demonstrated that arrow-headed design of velospheres enable rapid effective integration with electrospun matrices using arrow-mediated locking mechanism. Velosphers has been successfully cellularized with human adipose tissue derived stem cells using micromolded non-adhesive agarose hydrogel. Viability tests demonstrated high level of biocompatibility of cells inside tissue spheroid encaged into fabricated lockyballs and their capacity for spreading on synthetic electrospun matrices and tissue fusion into tissue constructs.

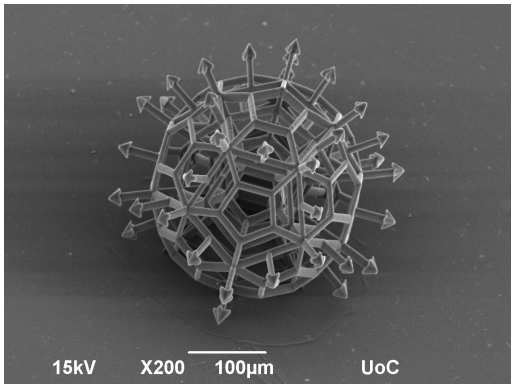

Figure 1. Scanning electron microscopy of arrow-headed microscaffold (velospheres) fabricated by two photon polymerization from photo-sensitive biomaterials

Conclusions

The new type of lockyballs family - arrow-headed lockyballs or simply velospheres has been designed and fabricated using two photon polymerization from photo-sensitive biometerials. Tissue spheroids encaged into arrow-headed velospheres are viable and their capacity for tissue fusion has not been compromised. Tissue spheroids encaged into velospheres can be rapidly attached to electrospun matrices by arrow-mediated locking mechanism and sequentially spread and fuse. This opens unique opportunities for rapid biofabrication into 3D tissue constructs using electrospun matrices interlocked by velospheres. Thus, arrow-headed lockyballs or velospheres represent another example of emerging third strategy in tissue engineering which allows to combine advantages of two main distinct premises in tissue engineering - conventional solid scaffold-based approach with bottom-up modular directed tissue self-assembly based approach and enable rapid biofabrication of 3D tissue constructs.

References

1. Kachouie N. et al. Organogenesis, 2010, 6 (4): 234-244.
2. Billiet T. et al. Biomaterials, 2012, 33 (26): 6020-6041.
3. Rezende R. et al. Virtual and Physical Prototyping, 2012, 7(4): 287-301.

Acknowledgements

This study was partly funded by Brazilian funding agencies CNPq and FAPESP and by FP7 Marie Curie ITN program TopBio.

Time-Resolved Imaging study of Laser-Assisted Bioprinting mechanism

Muhammad ALI[1], Aurélien FONTAINE[1], Alexandre DUCOM[1], Fabien GUILLEMOT[1]
[1] *Inserm U1026, Université Bordeaux Segalen, Bordeaux Cedex 33076, France*

Introduction

Laser Assisted Bioprinting (LAB) is a versatile, non-contact and nozzle free printing technique and has emerged as an alternative technology to fabricate two and three-dimensional tissue engineering products with high resolution patterns of biomaterials containing cells. The ejection dynamics of liquid jet of bioink by LAB has been investigated by Time Resolved Imaging (TRI)(Fig. 1). This study deals with the transition from sub-threshold to jetting conditions, what leads to mechanism insights which help next in controlling LAB conditions.

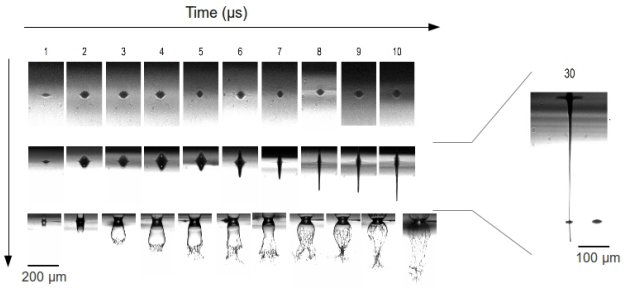

Figure 1. Time Resolved Imaging of laser-induced jet formation in LAB. a) First row represents sub-threshold regime, b) second row denotes jetting regime, c) third row shows plume regime, d) at the right hand, process of depositing droplet in jetting regime is shown.

Materials and Methods

Liquids used for these experiments were water based and (10 v/v%) glycerol solution with 1wt% alginate. Hydrogel film thickness was 40µm. The LAB process was initiated by a Nd:YAG laser (1064nm, 30ns) in single pulse mode. Time-resolved images from side view have been obtained by shadowgraphy. The jets initiated by Nd:YAG laser were illuminated by a second near IR pulse laser (810nm, 30ns) and captured by a CCD camera (resolution 1038x1388 pixels, via an optical zoom (Fig. 2).

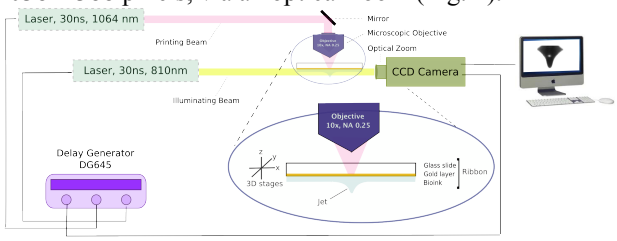

Figure 2. Time-Resolved Imaging set-up

Results and Discussion

In the sub-threshold regime, the vertex angle (Fig.3) of deformation was decreasing rapidly from 180° to 140° at 1µsec. During 1-4 µs the vertex angle decayed from 140° to 111°. The minimum vertex angle was 105° (Fig. 1a fifth frame) at 5µsec. From 6 µs, the vertex angle was observed to be increasing slowly (see graph Fig.4). Then the thriving bubble was being suppressed and the recoil had been started, afterwards oscillations were observed.

In case of the jetting- regime, the vertex angle of the front of the jet decreased apace during first few micro seconds from 180° to 144° at 1 µs. The quick expansion crossed critical limit of 105° and dropped to 96° at 2µsec and continued decreasing to 75° at 3 µs. The plateau observed during 3-4 µs (Fig. 4), indicates deviation from modelled curve. The further decrease in vertex angle was bit slow, 12.1° at 9 µsec. The slope of the graph in Fig. 4 is higher between 0-6 µs than during 6-10 µs. However, at 10µsec the vertex angle again increased to 17.9°.

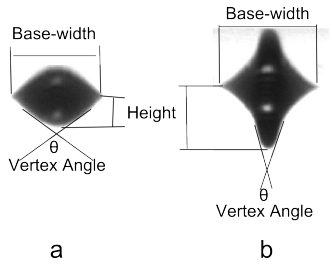

Figure 3. Definition of vertex angle for a) sub-threshold conditions and b) jetting conditions.

Figure 4. Evolution of vertex angle with time for different laser pulse energy

Interestingly, such angle value is in good agreement with the observations of Blake & Gibson[1] (104°) and the modelling completed by Longuet-Higgins [2] (109.5°) in the context of bubble cavitation close to free surface.

Conclusions

From these observations, printing parameters can be precisely tuned to ensure jet formation but minimizing stress applied to the materials printed.

References

1. Blake JR et al. Journal of Fluid Mechanics Digital Archive. 1981;111(-1):123–40.
2. Longuet-Higgins MS. Journal of Fluid Mechanics Digital Archive. 1983;127(-1):103–21.

Acknowledgements

ANR, HEC and Region Aquitaine for financial support.

Smart Scaffolds through Combination of Biofabrication Techniques

C. De Maria[1,2], G. Orsi[1], F. Montemurro[1], G. Criscenti[1], G. Vozzi[1,2]
Research Center E. Piaggio – University of Pisa, Pisa, Italy
Department of Ingegneria dell'Informazione – University of Pisa, Pisa, Italy

Introduction

A smart scaffold should combine right mechanical properties, micro and nano topology, appropriate biochemical cues. A combination of different materials, processed with different technology has the expectation to fulfill these requirements. In the present work we propose the combination of an extrusion-based system (PAM^2), and an inkjet printer (Penelope) to create a locally functionalized scaffold.

PAM^2 is a modular microfabrication system able to dispose high and low viscosity solution following precise spatial patterns. Temperature controlled reservoirs and deposition plate enable the fabrication of temperature sensitive biomaterials, while a laser pen allows to process photocurable polymers [1].

Penelope is a 3D thermal inkjet printer, based on HP technology, able to print several water-based solutions in a temperature controlled environment and with the possibility to print 3D object in with a layer-by-layer approach [2].

Combining these techniques we fabricated Polycaprolactone (PCL) based scaffolds functionalized using keratin hydrolysates precisely arranged onto the surface.

Keratins belong to the family of fibrous structural proteins and are the basic building blocks of feathers, hair and wool and the key structural materials of the outer layer of human skin and nails. Due to their unique chemical composition, biological activity and biocompatibility, keratins biomaterial is an appealing choice for therapeutic development. Keratins retain active cell binding motifs, such as LDV (Leu-Asp-Val) and RGD (Arg-Gly-Asp) binding sites, which are capable of supporting cellular adhesion and motility [3].

Materials and Methods

PCL (Sigma Aldrich) was solved in chloroform (Sigma Aldrich) 10% w/v and processed with PAM^2 system to fabricate squared grid scaffolds.

Functional groups were exposed dipping the scaffold into NaOH 2.5% (w/v) and SDS 0.05% (w/v) water solution for 2 hour, and then into EDC (2.5mM) and NHS (1mM) solution for 1 hour. Solutions of keratin hydrolysates at different percentages (from 0.5 to 10%) were printed using Penelope onto functionalized scaffold in precise positions. As control, functionalized scaffolds were dipped for 30 minutes in the same solutions.

Biological tests where performed using C2C12 mouse myoblast cell line. To discriminate the effects of material, geometry and decoration, cells were seeded, other than on previously described scaffolds, also on PCL film, on PCL scaffold, and on PCL film and scaffold functionalized and dipped into keratin solution for 30 minutes, printed PCL films. MTT and cell arrangement onto the scaffolds were evaluated. Paired T-test with a p-value of 5% was used for statistical analysis.

Results and Discussion

Inkjet printing of keratin solution was the more difficult step in the fabrication process, due to the changes in surface tension caused by keratin concentration: high concentrated solutions resulted into inhomogeneous results.

MTT results (fig.1) demonstrated that cells prefer functionalized substrates. The spotted decoration allowed to focus the presence of cells in a precise location an not on the whole surface. The presence of a complex geometry (with a subsequent larger surface area) seems to have an additive effects, giving the best results in terms of cell vitality.

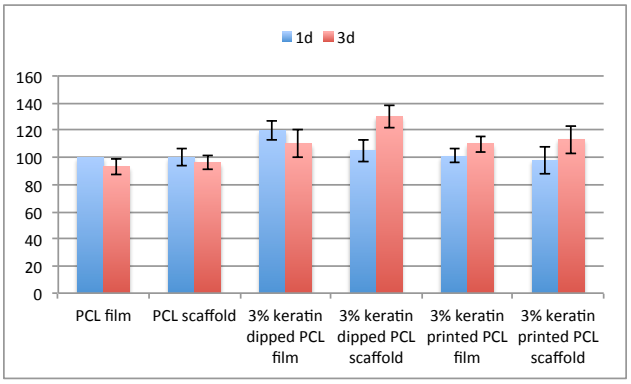

Figure 1. MTT results at 1 and 3 days

Conclusions

The presented combination of extrusion based systems, and inkjet printing joined mechanical properties, micro topology and biochemical cues. These combination can be further strengthened by the automated cell disposition ensured by inkjet printing.

References

[1] A Tirella, C De Maria, G Criscenti, G Vozzi, A Ahluwalia. The PAM^2 system: a multilevel approach for fabrication of complex three-dimensional microstructures Rapid Prototyping Journal 18 (4), 299-307

[2] C De Maria, J Rincon, AA Duarte, GVozzi, T Boland. A new approach to fabricate agarose microstructures Polym. Adv. Technol.. doi: 10.1002/pat.3162

[3]B Srinivasan, R Kumar, K Shanmugam, UT Sivagnam, NP Reddy, PK Sehgal. Porous keratin scaffold- promising biomaterial for tissue engineering and drug delivery. J Biomed Mater Res B Appl Biomater. 2010 Jan;92(1):5-12. doi: 10.1002/jbm.b.31483.

Shape Based Internal Architecture Modeling for Porous Tissue Scaffold

AKM B. Khoda*
Assistant Professor
Department of Industrial and Manufacturing Engineering
North Dakota State University
Fargo, ND 58102, USA

Ibrahim T. Ozbolat
Assistant Professor
Department of Mechanical and Industrial Engineering
CCAD, The University of Iowa,
Iowa City, IA 52242-1527, USA

Bahattin Koc
Associate Professor
Faculty of Engineering and Natural Sciences Sabanci University, Istanbul
34956, Turkey
bahattinkoc@sabanciuniv.edu

Introduction

In extrusion based additive manufacturing processes, one of the most common deposition patterns of making porous scaffolds is following a Cartesian layout pattern (0^0-90^0) in each layer crisscrossing the scaffold area arbitrarily as shown in Figure 1(a). In such structure, the porosity of designed scaffold do not conform the geometry of the replaced damaged tissue but simply approximates [1]. Besides, jumps or motion without deposition during their fabrication is also highly substantial due to the nature of the tool-path, which is independent of the geometry.

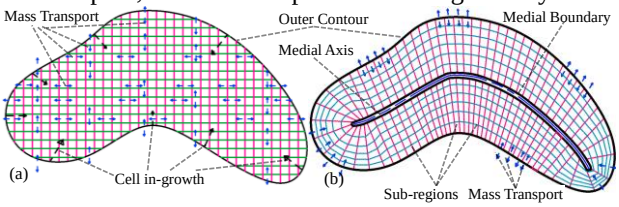

Figure 1 Mass transport and cell in-growth direction in (a) traditional layout pattern, and (b) proposed radial pattern.

Moreover, cells seeded in such uniform structure scaffold may have limited accessibility to the outer region for nutrient or mass in lieu of their locations i.e. accessibility via rectilinear filament distance (Figure 1a). This could affect the cell survival rate significantly [2]. However, a carefully crafted filament deposition between the outer contour and the medial region can improve the cell accessibility and may increase the mass transportation at any location as shown in Figure 1(b). A novel layer-based scaffold design is proposed to achieve functionally gradient variational porosity architecture. The designed layers have been optimized for a continuous, interconnected, and smooth material deposition path-planning for bio-additive fabrication processes.

Bio-modeling

The modeling technique has been proposed for layer-based additive manufacturing processes to control the internal architecture of tissue scaffolds. First, the anatomical 3D shape of the targeted region needs to be extracted using non-invasive techniques and layers are generated by slicing the 3D shape. To demonstrate the proposed heterogeneous controllable porosity modeling, two consecutive layers are considered as bi-layer pattern. For each layer, medial axis is constructed as the topological skeleton using inward offsetting method which is then converted into a two dimensional medial region.

The scaffolding area is discretized with radial ruling lines by connecting the boundaries of the medial region and the layer's outer contour. To increase accessibility, and to ensure the controllable smooth property transition between the outer and inner contours, an adaptive ruled layer algorithm is developed [3] and used. An optimization algorithm is developed [3] and sub-regions are accumulated from ruling lines. Dividing the sub-regions into pore-cell along their periphery generates iso-porosity regions for the consecutive layer. The combination of consecutive layers constructs the pore cells with desired pore sizes. Finally a continuous deposition path planning algorithm has been proposed to fabricate the designed scaffold with additive manufacturing techniques ensuring connectivity of the internal channel network shown in Figure 2.

Implementation

The proposed methodologies have been implemented with a 2.3 GHz PC using the Rhino Script and Visual Basic programming languages in the following examples. Two different scripts are written to implement the methodology on bi-layer pattern. The first script starts with the bilayer slice and generates the medial boundary. The second script uses the external and internal feature and generates the final tool-path performing all geometric algorithms sequentially. Time required to execute both script may vary based on the contour shape and desired gradient. However, required time can be reduced significantly by parallel processing or increasing the computational power.

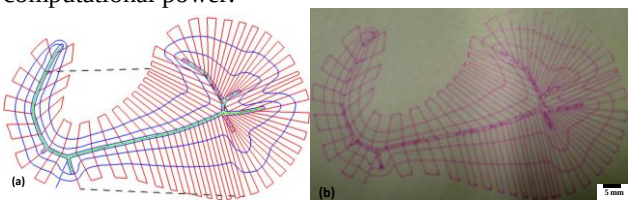

Figure 2 (a) Model and (b) fabrication for decreasing porosity gradient.

Conclusion

The proposed methodology can generates heterogeneous or gradient porosity through additive manufacturing techniques, either by changing the deposited filament diameter or by controlling the segment size i.e., the pore size during the fabrication processes.

References

[1] A. Khoda, I.T. Ozbolat, B. Koc, A functionally gradient variational porosity architecture for hollowed scaffolds fabrication, Biofabrication, 3 (2011) 1-15.
[2] F.P.W. Melchels, A.M.C. Barradas, C.A. Blitterswijk, J. Boer, J. Feijen, D.Grijpma, Effects of the architecture of tissue engineering scaffolds on cell seeding and culturing, Acta Biomaterialia, 6 (2010) 4208-4217.
[3] A.B. Khoda, I.T. Ozbolat, B. Koc, Designing Heterogeneous Porous Tissue Scaffolds for Additive Manufacturing Processes, Journal of Computer Aided Design (CAD), 2013 (In Press) http://dx.doi.org/10.1016/j.cad.2013.07.003.